A comparative study of neocortical development between humans and great apes

D I S S E R T A T I O N

zur Erlangung des akademischen Grades

Doctor of Philosophy
(Ph. D.)

vorgelegt

der Fakultät Mathematik und Naturwissenschaften
der Technischen Universität Dresden

von

Badsha, Farhath

geboren am 23. Juli 1986 in Chennai, India

Gutachter: Prof. Wieland B. Huttner
Prof. Christian Dahmann

Eingereicht am: 06.01.2017

Tag der Verteidigung: 05.04.2017

SUMMARY:

What makes us human? What drives our incessant need to keep asking ourselves that question? Is it our audacious claim of having superior cognitive abilities over all life forms (even though we have only ever known and experienced the world as a human) that pushes us to give our identity a meaning? Are other species as self-obsessed as we are? Where does obsession stem from? –the frontal lobe of the neocortex! The neocortex is one of the more recently evolved parts of the brain, which is largest in humans compared to any other known mammal– this could partly explain our above mentioned behaviour. Humans have evolved an expanded neocortex over the course of evolution through a massive increase in neuron number (compared to our close relatives- the chimpanzees) in spite of sharing similar gestation time frames. So what do humans do differently compared to chimpanzees within the same time frame during their development? This dissertation addresses this question by comparing the developmental progression of neurogenesis between humans and chimpanzees using cerebral organoids as the model system.

Although, we are yet far from being able to re-create the brain– human or otherwise, in all its complexity, recent progress in science has enabled us to develop *in vitro* model systems derived from pluripotent stem cells, called cerebral organoids, which recapitulate the development of the mammalian brain. The usage of cerebral organoids, has enabled us to compare the development of both the human neocortex, and the chimpanzee neocortex from the very initiation of the neural phase of embryogenesis until very long periods of time.

An attempt was also made to study the orangutan neocortical development, however, this study needed further optimization.

The results obtained so far suggest that the genetic programs underlying the development of the chimpanzee neocortex and the human neocortex are not very different, but rather the difference lies in the timing of the developmental progression. These results show that the chimpanzee neocortex spends lesser time in its proliferation phase, and allots lesser time to the generation of its neurons than the human neocortex. In more scientific terms, the neurogenic phase of the neocortex is shorter in chimpanzees than it is in humans. This conclusion is supported by (1) an earlier onset of gliogenesis in chimpanzees compared to humans which is indicative of a declining neurogenic phase, (2) an earlier increase in the chimpanzee neurogenic progenitors during development, compared to humans, (3) a higher number of stem cell– like progenitors in human cortices compared to chimpanzees, (4) a decline in neurogenic areas within the chimpanzee cerebral organoids over time compared to human cerebral organoids.

Given that all types of cortical progenitors originate from the initial PAX6+ apical neural stem cell– like progenitors, it would be interesting to study and compare the lineage progression of these progenitors between the two species over time, with a follow up quantitative study of the early, mid and late born neurons, in order to better understand the earlier gliogenic switch in chimpanzee cortices compared to human ones.

LIST OF ABBREVIATIONS:

AP : Apical progenitor
BP : Basal progenitor
bRG : Basal radial glia
BLBP : Brain lipid binding protein
CNS : Central nervous system
COL V : Collagen V
CP : Cortical plate
CSF : Cerebral spinal fluid
DCX : Doublecortin
ECM : Extracellular matrix
EdU : Ethynyl deoxyuridine
ESC : Embryonic stem cells
GABA : Gamma-aminobutyric acid
GFAP : Glial fibrillary acidic protein
GFP : Green fluorescent protein
GLAST : Glutamate aspartate transporter
iPSC : Induced pluripotent stem cells
INM : Interkinetic nuclear migration
ISVZ : Inner subventricular zone
IUE : *In utero* electroporation
NEC : Neuroepithelial cells
NPC : Neural progenitor cells
OLIG2 : Oligodendrocyte transcription factor 2
OSVZ : Outer subventricular zone
PAX6 : Paired box-6
PBS : Phosphate buffer saline
PH3 : Phosphohistone H3
pVIM : Phosphovimentin
SATB2 : Special AT-rich sequence-binding protein
SOX : Sry box
SVZ : Subventricular zone
TAP : Transit amplifying progenitors
TBR : T-brain
tbRG : Transient basal radial glia
TF : Transcription factor
TUJ1 : ß III tubulin
VZ : Ventricular zone

LIST OF FIGURES:

1. Human embryogenesis
2. Germ layer differentiation
3. Progression of neocortical development
4. Model system- cerebral organoid
5. Human cerebral organoid characterization at day 30
6. Features at the cortical apical boundary
7. Data showing similar gene expression profiles characterize lineage progression in organoid and foetal cerebral cortex
8. Extracellular matrix lining cortical regions
9. Orangutan cerebral organoids
10. Comparison between human and chimpanzee cerebral organoid marker expression
11. Chimpanzee cerebral organoids recapitulate cortex development
12. Earlier onset of gliogenesis in chimpanzee organoids
13. Later stages of neurogenesis showing S100β glial marker expression
14. Gliogenesis in human cerebral organoid cortices
15. Comparison of proliferative progenitors between human and chimpanzee cerebral organoid cortices
16. Estimation of cell cycle re-entry of organoid cortical progenitors
17. Schematic representation of the cumulative EdU labeling experiment
18. Determination of cell cycle parameters of human and chimpanzee organoid APs (PAX6+TBR2−) using cumulative EdU labeling
19. Determination of cell cycle parameters of human and chimpanzee organoid BPs (PAX6+TBR2+) using cumulative EdU labeling
20. Determination of cell cycle parameters of human and chimpanzee organoid BPs (PAX6−TBR2+) using cumulative EdU labeling
21. Changes in the proportion of cortical NSPC subtypes and neurons during human and chimpanzee cerebral organoid development
22. Quantification of PAX6+TBR2+ cells in VZ
23. Quantification of cortical neuron number at D52 human and chimpanzee cerebral organoids
24. Gene ontology enrichments (-log10 P-value) for differentially expressed gene groups
25. Differences in number of mitotic cells in human and chimpanzee cerebral organoids
26. Electroporation of a cerebral organoid

LIST OF TABLES:

1. Media and reagents tried and tested for generating cerebral organoids

CONTENTS:

1. Introduction……1
1.1. Vertebrate embryogenesis……2
1.2. Development of the mammalian brain……4
1.2.1. The neocortex and its development……5
1.2.1.1. Cortical neurons……6
1.2.1.2. Germinal Zones……7
1.2.1.3. Progenitors……8
1.2.1.4. Glia……11
1.2.2. Neurogenic length and cell fate determinants……12
1.3. Model system- cerebral organoid……13
1.3.1. Organoid development mimics the development of the mammalian brain……13
1.3.1.1. Organoid "embryogenesis"……13
1.3.1.2. Organoid neocortical development……15

2. Results……17
2.1. Optimization of the protocol……18
2.2. Characterization of human cerebral organoids based on marker expression……19
2.2.1. Study of the progression of neurogenesis in cerebral organoid dorsal cortex using immunofluorescence……22
2.2.2. Transcriptome analysis- Gene expression in human foetal cortex vs human cerebral organoid cortex……24
2.3. Characterization of chimpanzee and orangutan cerebral organoids based on marker expression……27
2.3.1. Comparison of the progression of neurogenesis in chimpanzee cerebral organoid to that observed in the human cerebral organoid……29
2.3.2. Transcriptome analysis- Gene expression in chimpanzee cerebral organoid cortex……30
2.4. Comparison between development of human and chimpanzee cerebral organoids……32
2.4.1. Comparison of progression of neurogenesis between the dorsal cortices of human cerebral organoids and chimpanzee cerebral organoids……33
2.5. Factors influencing longer neurogenic period in human cerebral organoid cortices compared to chimpanzee organoid cortices……38
2.5.1 Analysis of the proliferative capacity of human and chimpanzee cortical progenitors……38
2.5.1.1. Estimation of the total number of proliferating cortical progenitors between human and chimpanzee cerebral organoids……39
2.5.1.2. Estimation of the number of actively cycling cortical progenitors between human and chimpanzee cerebral organoids……40

2.5.2. Cell cycle lengths analysis and their differences between human and chimpanzee cortical progenitors……41
2.5.2.1. Cell cycle length of apical progenitors (PAX6+TBR2– cells)……42
2.5.2.2. Cell cycle length of basal progenitors (PAX6+TBR2+ cells)……43
2.5.2.3. Cell cycle length of basal progenitors (PAX6–TBR2+ cells)……44
2.5.3. Comparison between human and chimpanzee organoid cell composition……45
2.5.4 Differential gene expression between human and chimpanzee cerebral organoids……50
2.6. Other differences found between human and chimpanzee cerebral organoids……51

3. Discussion……55
3.1. Cerebral organoids as a model system……56
3.2. Cortical cell diversity in cerebral organoids……58
3.3. Differences in cortical cell composition between human and chimpanzee organoids reflects a more neurogenic fate for chimpanzee PAX6+TBR2– NSPCs……59
3.4. Cell cycle characteristics of human and chimpanzee organoid cortical progenitors suggest a higher proliferative capacity for human PAX6+TBR2– NSPCs……61
3.5. Gene expression studies of organoid cortical cells reflect inherent evolutionary adaptations……62
3.6. Neurogenic length of human organoid cortices is longer than that of chimpanzee organoid cortices……63

4. Materials and methods……66
4.1. Materials……67
4.1.1. Cell lines……67
4.1.2. Cell culture components……67
4.1.3. Other reagents and chemicals……68
4.1.4. Organoid culturing solutions and media……69
4.1.5. Buffers and mounting media……70
4.1.6. Primary antibodies……70
4.1.7. Secondary antibodies……71
4.2. Methods……72
4.2.1. Cell line culturing and maintenance……72
4.2.2. Organoid culturing and maintenance……73
4.2.2.1. Embryoid body formation……73
4.2.2.2. Neural Induction……73
4.2.2.3. Development of the neuroepithelium……73
4.2.3. Organoid processing……74
4.2.3.1. Organoid Fixation……74

4.2.3.2. Cryosectioning……75
4.2.4. Immunofluorescence……75
4.2.5. Cumulative EdU labeling and detection……76
4.2.6. EdU pulse chase experiment……77
4.2.7. Single cell RNA sequencing experiments and analyses……77
4.2.8. Image acquisition and analysis……78
4.2.9. Statistical analysis……78
4.3. Tried and tested……78
4.3.1. Other organoid media……78
4.3.2. Electroporation of cerebral organoid……79

5. References……82

6. Appendix……96
6.1. List of publications (from thesis work)……97
6.2. List of manuscripts in preparation……97
6.3. Conference attendance……97

Acknowledgements……98

Declaration……100

1. Introduction

1.1. VERTEBRATE EMBRYOGENESIS:

"And certainly did We create man from an extract of clay. Then We placed him as a sperm-drop in a firm lodging. Then We made the sperm-drop into a clinging clot, and We made the clot into a lump [of flesh], and We made [from] the lump, bones, and We covered the bones with flesh; then We developed him into another creation. So blessed is Allah, the best of creators." – Al Qur'an, 23:12-14.

After the fusion of the male and female nuclei during fertilization, cleavage begins, wherein the cells undergo a number of mitotic divisions resulting in a reduction of cell size with increase in cell number within the **zygote**. These cells, at this point, are **pluripotent**, meaning they are capable of generating any tissue type. After multiple mitotic division cycles, the cells (now collectively termed as the embryo) form a **blastocyst** that consists of a group of cells surrounding a central fluid filled cavity (the blastocoel) (Figure 1). The blastocyst then undergoes gastrulation resulting in the initiation of germ layer differentiation (Figure 2).

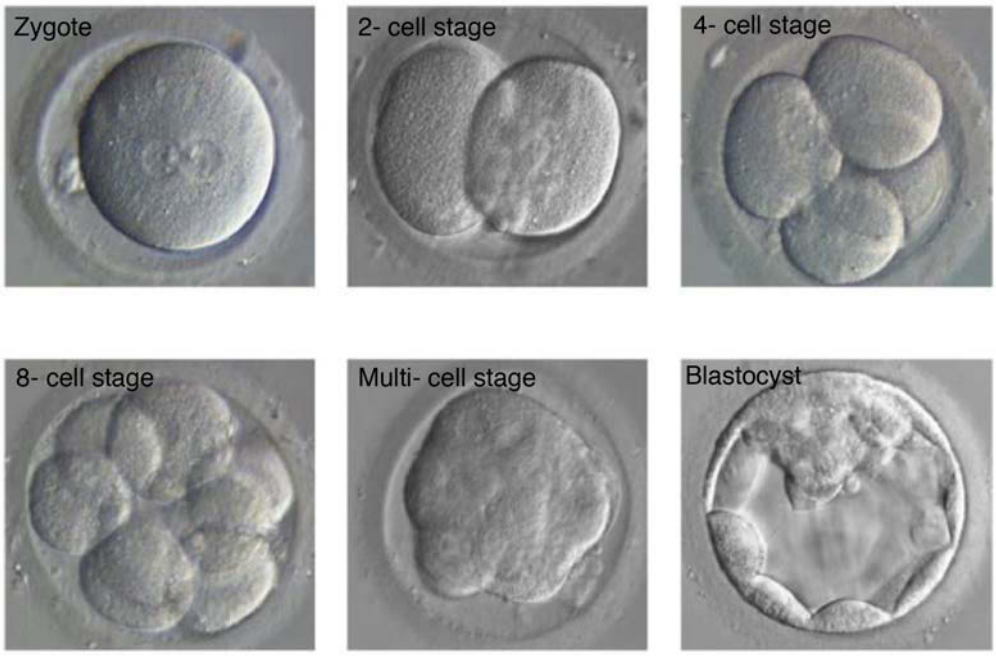

Figure 1. Human embryogenesis: Initial phase showing the transition of the zygote through the various mitotic stages until the formation of the blastocyst (Courtsey: modified from Dr. Kathy Niakan).

Simplistically put, as the embryogenesis proceeds further into late gastrulation, the germ layers- ectoderm, mesoderm and endoderm become more prominent and re-arrange themselves into an outer layer (**ectoderm**), the middle layer (**mesoderm**) and an inner layer (**endoderm**) (Figure 2). The ectoderm eventually gives rise to the central nervous system and the epidermis, while the mesoderm gives rise to muscle, bone, cartilage, blood and internal organs such as the heart, and kidney. The endoderm, the inner most layer gives rise to the gut, lungs and liver.

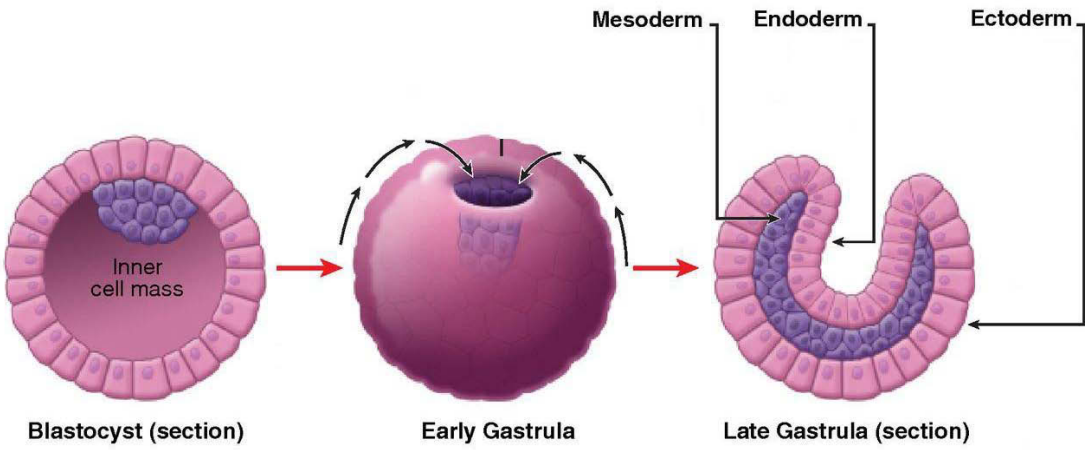

Figure 2. Germ layer differentiation: Cells from the epiblast undergo an epithelial to mesenchymal transition and ingress at the primitive streak to form the three germ layers (Modified from Berardi et al., 2012).

During the course of embryogenesis, the ectoderm forms a **neural plate**, which further folds to form the **neural tube** consisting of a layer of neuroepithelial cells surrounding a fluid filled cavity. Further growth and differentiation of these **neuroepithelial cells** into various progenitor, neuronal and glial cell types and their self-organization and patterning gives rise to the mammalian brain in all its complexity.

1.2. DEVELOPMENT OF THE MAMMALIAN BRAIN:

The neuroepithelial cells of the neural tube undergo repeated proliferation to form a large pool of varying progenitor cell types, which then ultimately produce the three-vesicle enclosing, brain regions- the **prosencephalon** (the forebrain), the **mesencephalon** (the mid brain) and the **rhombencephalon** (the hind brain). The prosencephalon can be further divided into the **telencephalon** and the **diencephalon**. The telencephalon is the region that eventually develops into

the **cerebral cortex**, which can be further broadly divided into the **neocortex** and the **allocortex**. The neocortex is considered to be the most recently evolved part of the cerebral cortex and the primary focus of this study. The increasing intelligence along the evolutionary tree leading to man is largely attributed to the development and changes that have occurred and accumulated in the neocortex over the course of evolution.

1.2.1. The neocortex and its development:

The neocortex (also known as the neopallium or the isocortex) is the largest portion of the cerebral cortex. It consists of **six horizontal layers**, the innermost layer being layer VI and the outermost layer being layer I. The layering of the neocortex is mostly based on the type of cells localizing a given longitudinal area. The neocortex can also be divided into **functional cortical columns** (vertical areas across all six layers) involved in a common function (Greig et al., 2013). In adult mammals, the neocortex consists of the **outer grey matter** comprising the neuronal cell bodies, dendrites, astroglia, oligodendrocytes, unmyelinated axons and synapses, and the **inner white matter** comprising the myelinated axons.

In primates (except the marmoset), the neocortex is folded into ridges known as "**gyri**" and grooves called "**sulci**". Animals that possess a folded neocortex are said to be **gyrencephalic** as opposed to those with a smooth neocortex (**lissencephalic**). One of the theories for the existence of gyrification is an increased number of neurons that need to be accommodated within the limited space of a skull. This increase in neuron number is also attributed to the

increased intelligence observed in one species compared to another, e.g., humans (~20 billion neurons) vs chimpanzees (~6 billion neurons) (Lewitus et al., 2014).

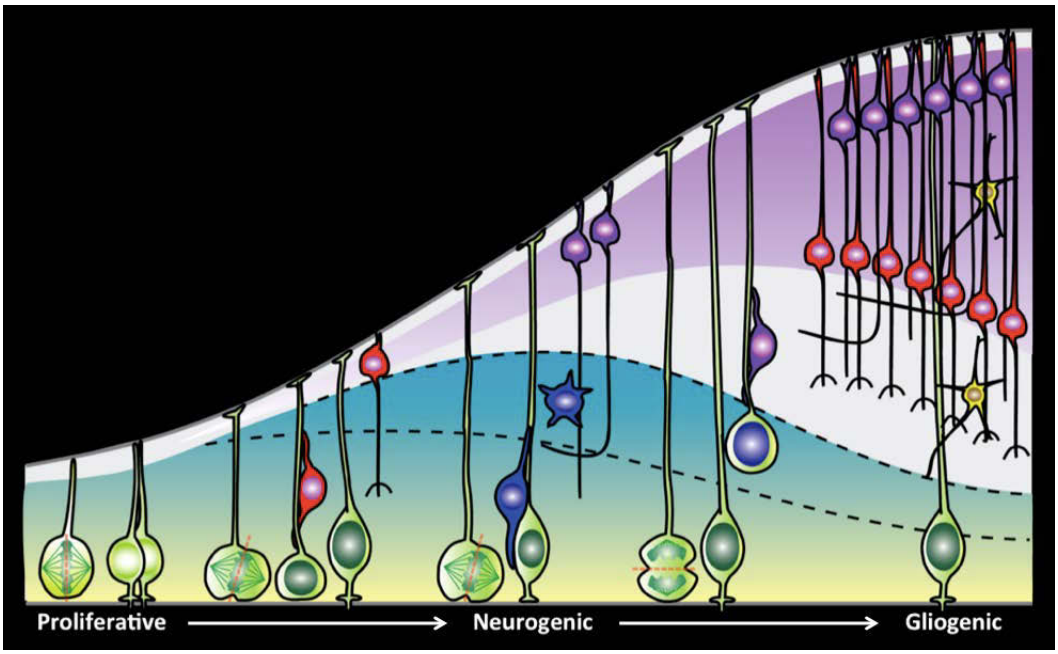

Figure 3. Progression of neocortical development: Early (proliferative) phase resulting in the increase in progenitor cell population, mid (neurogenic) phase resulting in more neurogenic progenitors and neurons, and late (gliogenic) phase wherein, neuron production begins to decline with a shift toward glial cell production. Progenitors in green, early born neurons in red, neurogenic progenitors in blue/green, late born neurons in purple and astrocytes in yellow (Graphic originally created by Dr. Yoon Jeung Chang).

1.2.1.1. Cortical neurons:

The cortical neurons comprise of two principal classes of neurons: the inhibitory, GABAergic local **interneurons** and the excitatory, glutamatergic **projection neurons**. Most of the interneurons originate from the ventral telencephalon and migrate toward the dorsal telencephalon (layer IV), however

in humans, a few of these interneurons also originate from within the dorsal telencephalon (Anderson et al., 1997; Hansen et al., 2013; Ma et al., 2013). In contrast, the projection neurons originate from the dorsal telencephalon and project their axons to other parts of the cerebral cortex.

The cortical projection neurons are broadly classified into three categories based on their axonal extension 1) within the cortical hemisphere- "**associative projection neurons**" (layer IV granular neurons), 2) across the midline to the other hemisphere- "**commissural projection neurons**" (layers II, III, V, VI callosal projection neurons), or 3) away from the cortex- "**corticofugal projection neurons**" (layer VI corticothalamic projection neurons, layer V subcerebral projection neurons) (Greig et al., 2013). In addition to these neurons, layer I (or the "**marginal zone**") houses the earliest born neurons named the **Cajal- Retzius cells** (Bystron et al., 2006). The Cajal- Retzius cells secrete **reelin**, which plays a role in the radial migration of neurons along the radial glial processes (Aboitiz et al., 2001). During mammalian neurogenesis, the neurons of the neocortex arrange themselves in an inside-out fashion, with the early born neurons occupying the deep layer VI, followed by layer V, and the later born neurons occupying the upper layers IV, III and then II (Molyneaux et al., 2007).

1.2.1.2. Germinal zones:

The projection neurons populating the different layers of the neocortex are derived from the progenitor cells situated in two germinal zones situated at the base of layer VI of the neocortex. The layer that is in immediate contact with

layer VI is the "**intermediate zone**" (IZ) below which is the "**sub ventricular zone**" (SVZ) and the layer below the SVZ (i.e., the layer lining the lateral ventricle) is called the "**ventricular zone**" (VZ). In gyrencephalic mammals like humans and apes, the SVZ is expanded, and further divided into an inner SVZ (**iSVZ**) and an outer SVZ (**oSVZ**) (Smart et al., 2002).

During embryonic development, the neuroepithelial cells lining the ventricle of the neural tube form the initial ventricular zone, and with the onset of neurogenesis, these neuroepithelial cells transition to a radial glial state, proliferate and differentiate into various types of progenitors, neurons and glia, which then occupy the VZ, the SVZ and the cortical plate (Figure 3).

1.2.1.3. Progenitors:

The development of the mammalian brain begins with the enclosing of vesicles by a layer of **neuroepithelial cells** that form the neuroepithelium. These cells are bipolar, having both an apical and basal process contacting the apical and basal surfaces respectively, undergo symmetric proliferative divisions (they produce two identical daughter neuroepithelial cells), and have a high capacity for self- renewal.

Even though the neuroepithelium comprises of a single layer of cells, it has a stratified appearance owing to a phenomenon called interkinetic nuclear migration (INM) wherein the neuroepithelial cells undergo mitosis at the apical surface but move basally during their G1 phase, undergo S-phase basally and traverse back to the apical surface during their G2 phase (Taverna and Huttner,

2010), thus the cell bodies of these neuroepithelial cells are distributed all through the cortical wall creating the illusion of multiple layering of cells, referred to as pseudostratification (Sauer, 1935; Messier, 1978; Takahashi et al., 1993; Götz and Huttner, 2005;).

With the onset of neurogenesis, the neuroepithelial cells down regulate their tight junctions (Götz and Huttner, 2005) and gain a glial identity by expressing glial markers such as glutamate aspartate transporter (GLAST) and brain lipid binding protein (Kriegstein and Álvarez-Buylla, 2009). These cells, now termed **radial glia**, have similar properties as the neuroepithelial cells in the sense that they are bipolar, have both apical and basal contacts and undergo INM. They initially undergo symmetric proliferative divisions, but as neurogenesis progresses, they switch to an asymmetric division mode resulting in one daughter being a radial glial cell and the other daughter being either a differentiated progenitor or a neuron (Takahashi et al., 1996; Götz and Huttner, 2005). There is another poorly understood set of cells, previously called **short neural precursors**, which maintain their apical contact but not their basal contact and are different from the apical radial glia by their expression of Tα1 promoter (Gal et al., 2006; Florio and Huttner, 2014). These cells undergo symmetric consumptive divisions resulting in the production of two neurons. Collectively, the cells that maintain contact with the apical surface, undergo mitosis at the apical surface and express prominent markers such as PAX6 (Götz et al., 1998) and Prominin-1 (Weigmann et al., 1997) are broadly termed as **apical progenitors**. The apical progenitors that have adopted a neuronal fate

(producing a neuron via the next generation of daughter cells) express the transcription factor TIS21.

Following asymmetric cell division, one daughter cell of the apical radial glia remains an apical radial glia whereas the other daughter cell delaminates, loses contact with the apical surface and migrates basally thus giving rise to a range of **basal progenitors** which then occupy the **SVZ**.

Basal progenitors (as in the case of primates) may either be non-polar (basal intermediate progenitor; **bIP**), or have only a basal process contacting the basal surface (basal radial glial- basal P; **bRG- basal- P**), or have only an apically directed process not in contact with the apical surface (**bRG- apical- P**), or have both apical and basal processes but with only the basal contact (**bRG- both- P**) or have transiently expressing apical and basal processes without contact with either apical or basal surfaces (transient basal radial glia; **tbRG**) (Betizeau et al., 2013). These cells express the transcription factor TBR2, undergo both asymmetric self-renewing cell divisions and symmetric proliferating divisions (in primates) (Hansen et al., 2010; LaMonica et al., 2013; Betizeau et al., 2013, Florio and Huttner, 2014), a characteristic that is believed to be responsible for the increasing cortical neuron number associated with gyrencephaly and intelligence over the course of evolution. Basal progenitors do not undergo INM but exhibit a rapid apical or basal movement referred to as “mitotic somal translocation” prior to cytokinesis.

Apart from these cells, there is another group of non- polar cells in the basal compartment, called the **transit- amplifying progenitors (TAPs)** that have a high self-renewal capacity (Lui et al., 2011) and undergo multiple rounds of symmetric proliferative divisions before generating neurons (Noctor et al., 2004; Hansen et al., 2010; LaMonica et al., 2013). These cells express both TBR2 as well as PAX6 transcription factors (Fietz et al., 2010; Betizeau et al., 2013).

1.2.1.4. Glia:

Glial cells are non- neuronal cells that provide support and protection to the neurons in the CNS (and also the neurons of the peripheral nervous system) by producing myelin, maintaining homeostasis, clearing dead neuronal cells and fighting pathogens. There are different types of glial cells in the CNS namely, **microglia** and **macroglia** (astrocytes, oligodendrocytes and ependymal cells). The macroglia are derived from the ectoderm, whereas, the microglia have a mesenchymal origin. Glia are known to undergo mitosis unlike neurons, which are believed to be post mitotic. During late neurogenesis, the radial glial cells switch cell fate to that of macroglia possibly by expressing SOX9 as observed in the developing spinal cord (Stolt et al., 2003). These macroglia, while residing in the cortical plate, play an important role in axonal insulation, synaptic plasticity and transmission. They are positive for GFAP but negative for neuronal markers. Certain mature astrocytes (such as the ones ensheathing blood vessels) and oligodendrocytes express S100β at later stages of development.

1.2.2. Neurogenic length and cell fate determinants:

The final output of neurons and the general complexity of the neocortex is dependent on the length of the neurogenic phase of a species. The neurogenic length is in turn dependent on the nature and fate of the progenitor cells present in the developing neocortex. The cell fate of the progenitor cells can be influenced by extrinsic factors such as the extracellular matrix (ECM), contact with factors in the cerebrospinal fluid (CSF), or the basal lamina, secreted factors between cells etc., or by intrinsic factors such as inherent transcriptional programs, presence or absence of certain factors (e.g., apical complex) or by their cell biological characteristics such as the mode of cell division, spindle orientation or the length of cell cycle (Lehtinen and Walsch, 2011; Kelava et al., 2012; Paridean and Huttner, 2014). Even a difference in the length of the individual phases of the cell cycle are known to contribute to fate determination, e.g., proliferative progenitors have been shown to have longer S- phase compared to neurogenic progenitors (Arai et al., 2011).

Computational predictions have shown that humans may have a longer neurogenic phase than great apes (Lewitus et al., 2014), which might explain the higher neuronal output seen in humans when compared to great apes (~21 billion neurons in adult humans compared to 6.2 billion neurons in adult chimpanzees). This thesis explores the possibility of such a scenario using stem cell derived **cerebral organoids** as the model system.

1.3. MODEL SYSTEM- CEREBRAL ORGANOID:

Recent advances in science have enabled the production of self-organizing structures reminiscent of the developing brain from pluripotent stem cells (embryonic stem cells, ESCs or induced pluripotent stem cells, iPSCs), presenting a unique opportunity to model cerebral organoid development in vitro. These cerebral organoids are generally heterogeneous and allow the formation of a variety of brain-like regions including the cerebral cortex, ventral forebrain, midbrain– hindbrain boundary, and hippocampus.

The protocol to grow cerebral organoids (Lancaster et al., 2013) was designed to mimic early stages of human dorsal cortical brain development by relying on the intrinsic self-organizational capacity of the cells to pattern, specify, and generate structured cerebral tissue. This protocol establishes cortical-like tissue with compartmentalized germinal zones including a VZ, SVZ and a cortical plate.

1.3.1. Organoid development mimics the development of the mammalian brain:

1.3.1.1. Organoid "embryogenesis":

As in the development of a vertebrate embryo, wherein the pluripotent cells of the embryo differentiate and give rise to the germ layers- ectoderm, mesoderm and endoderm, which later become specified to form different parts of the body, the dissociated pluripotent stem cells suspended in a low attachment 96 well plate also aggregate together to form an embryoid body, which eventually differentiates to form the three germ layers (Figure 4). Of these, the ectoderm

adopts a neural lineage, as is expected in the absence of extrinsic influences (Smukler et al., 2006). Upon neural induction, these embryoid bodies are allowed to grow in an environment that supports and promotes neuroepithelial development.

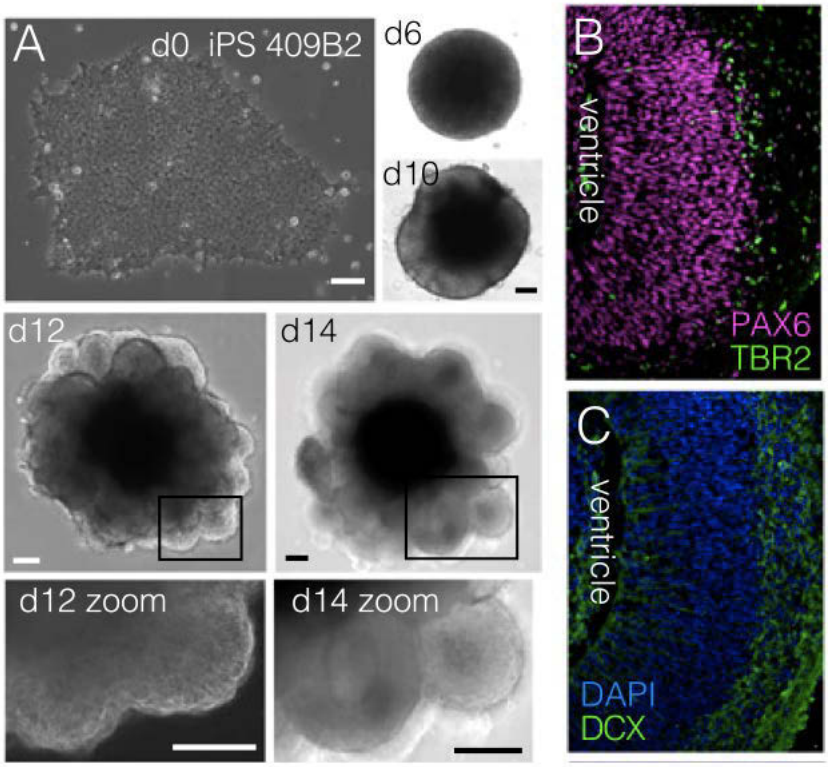

Figure 4. Model system- cerebral organoid (Modified from Camp, Badsha et al., 2015)**:**

(A) Images from various stages of cerebral organoid development. Top panel: from left to right, iPSC colonies, embryoid bodies (D6), neural induction (D10); middle panel: from left to right, 2 days after matrigel embedding (D12), 4 days after matrigel embedding (D14); bottom panel: left to right, insets showing stratified epithelium surrounding a ventricle in D12 and D14 organoids respectively. Boxes indicate areas shown at greater magnification, as indicated. (Scale bars, 100 μm).

(B) Cortical region from 35 days old organoid immunostained for neural markers, PAX6 (magenta) and TBR2 (green).

(C) Cortical region from 35 days old organoid immunostained for neuronal marker, DCX (green), and DAPI (blue).

1.3.1.2. Organoid neocortical development:

The neuro-ectoderm of the embryoid body forms tiny folds or buds, containing neuroepithelial cells enclosing a ventricle (Figure 4), similar to the neural tube enclosing a fluid filled cavity in a developing embryo. And just as in the developing neuroepithelium, the apical progenitors of the VZ line a lumen, express radial glial marker genes (Figure 4), undergo interkinetic nuclear migration, and divide at the apical surface. In addition, time-lapse microscopy and immunostainings have revealed patterns of direct and indirect neurogenesis in an abventricular location, reminiscent of the SVZ containing basal progenitors albeit in lesser abundance than in the in vivo human neocortex. During the course of their development, the cerebral organoids eventually form a cortical plate, which (due to the protocol used) is not clearly differentiated into its characteristic six layers (Lancaster et al., 2013). The observations of a cortical architecture, cellular behavior based on marker gene expression and bulk transcriptome analysis are generally consistent with in vivo patterns of human foetal cortical development.

Thus, the cerebral organoid was deemed a suitable model system to study and compare the course of neocortical development in humans and great apes.

2. RESULTS

2.1. OPTIMIZATION OF THE PROTOCOL:

In order to study and compare the development of human and non-human primate neocortices using cerebral organoids, several iPSC lines from each species (both commercial and from collaborators) were tried and tested using the protocol established by Madeline Lancaster (Lancaster et al., 2013; Lancaster and Knoblich, 2014). About five human lines (one ES cell line, four iPS cell lines), five chimpanzee lines (iPS cell lines) and one orangutan line (iPS cell line) were tested.

Either due to the differences in the reprogramming protocol or due to the inherent nature of the cell lines, not all lines tested yielded similar results. Hence the Lancaster protocol was modified step by step to establish a common protocol that could be used for a majority of cell lines. Some of these cell lines did not show proper iPSC colony behavior while others did not undergo proper germ layer differentiation resulting in a mass of undefined cells upon neural induction and differentiation.

To overcome this, first, the cell lines that did not show proper iPSC behavior or the lines that showed a higher degree of spontaneous differentiation were eliminated from the study. Next, various combinations of media were tested to achieve optimal embryoid body formation and differentiation across different cell lines (details of such trials and fails are discussed at the end of the dissertation under "Tried and Tested"). In the end, only six cell lines (three human, two chimpanzee and one orangutan) were used with a common modification in the first step (formation of embryoid bodies) wherein, the

embryoid bodies (EBs) were generated using mTeSR1 medium instead of the low bFGF hESC medium. This helped some of the iPSC lines to form healthier EBs that could further undergo proper germ layer differentiation. Apart from this, the EBs were allowed to grow in mTeSR1 until the appearance of the germ layers rather than adhering to the timeline and the light microscopy guidelines specified in the Lancaster protocol. Upon formation of the germ layers, however, the timeline was kept constant for all other steps (involving the development of the whole organoid) within batches and between different lines used in the same batch. This was done in order to enable the comparison of cortical development and its progression between cerebral organoids from different species.

For further comparative studies, only three human cell lines (H9 feeder free, 409B2, SC102A1) and two chimpanzee cell lines (Sandra A, PR818-5) were used. The organoids produced by the orangutan cell line (Toba) were not optimal and were thus excluded from studies involving quantification. All cell lines were tested for pluripotency marker expression and chromosomal aberrations.

2.2. CHARACTERIZATION OF HUMAN CEREBRAL ORGANOIDS BASED ON MARKER EXPRESSION:

As a first step, the human cerebral organoids made, using the Lancaster protocol, from the human pluripotent cell lines mentioned above, were validated to ascertain the reproducibility of the protocol. In order to do so, these cerebral organoids were subjected to immunofluorescence and single cell transcriptomics so as to obtain a dual confirmation of the spatiotemporal expression of the marker proteins and their genes.

Unlike in the case of the human neocortex, the germinal zones of the cerebral organoid (made with the Lancaster et al., 2013 protocol) could be distinguished clearly from one another only to a certain extent, in that, only the ventricular zone (VZ) could be clearly visualized due to its distinct pseudostratification using DAPI alone. The other layers of the cortical wall, such as the sub-ventricular zone (SVZ) and the cortical plate (CP) could only be visualized using specific markers such as TBR1, DCX for neurons (CP) and TBR2 for neurogenic progenitors residing between the cortical plate and the ventricular zone (the putative SVZ). Hence all analysis and quantifications were done based on the expression of the markers to define the cell type rather than by zone demarcations. These markers were used to distinguish between neural stem-like progenitors, neurogenic progenitors and neurons.

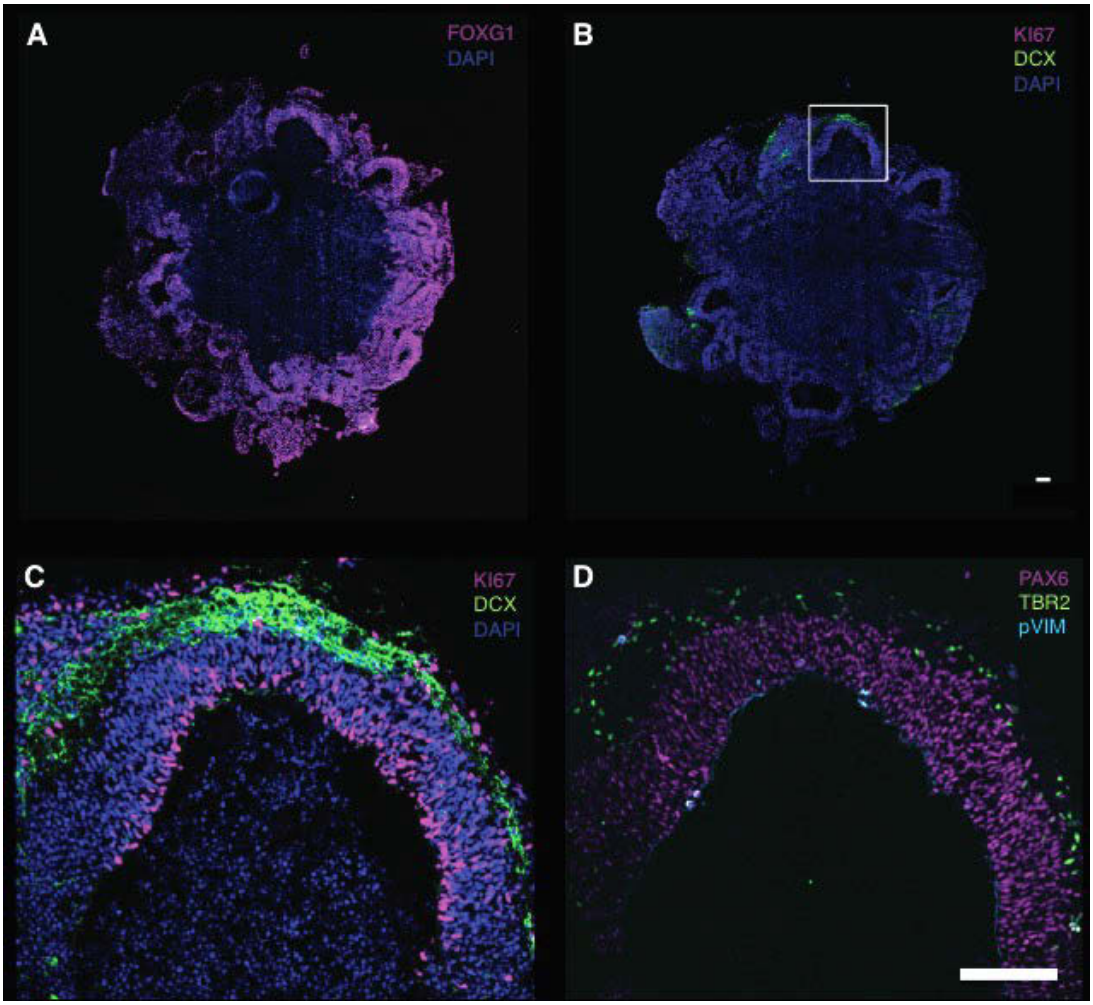

Figure 5. Human cerebral organoid characterization at day 30: The cerebral organoid is stained for-

(A) Forebrain marker FOXG1 (magenta) and DAPI (blue); (B) Proliferating progenitor marker KI67 (magenta), neuronal marker DCX (green) and DAPI (blue); white box shows area of magnification of a single ventricle- shown in (C); (D) Single ventricle stained for apical progenitor marker PAX6 (magenta), basal progenitor marker TBR2 (green) and mitotic cell marker pVIM (cyan). (Scale bars, 100 μm).

2.2.1. Study of the progression of neurogenesis in cerebral organoid dorsal cortex using immunofluorescence:

Human cerebral organoids across different batches were tested at different time points to check for proper progression of neural development and the presence of the area of interest (dorsal cortex) using antibodies against markers of forebrain such as FOXG1, neural stem cells and neurogenic progenitor markers such as PAX6 and TBR2 respectively, along with neuronal markers such as DCX. Other neuronal markers such as TBR1, CTIP2 and SATB2, which are expressed during early, mid, and late stages of neurogenesis, respectively (Greig et al., 2013), were used to ascertain the degree of progression of neurogenesis.

These cerebral organoids formed complex tissue structures that resembled the developing primate brain, as reported previously for human cerebral organoids (Lancaster et al., 2013). They showed cortex-like FOXG1 positive regions (Figure 5A) with PAX6+ APs (like radial glia) residing predominantly in the apical-most zone facing a ventricular lumen (Figure 5B), similar to the ventricular zone (VZ) of developing primate neocortex at an early-mid stage of neurogenesis. Consistent with this, cells immunoreactive for the neuron marker DCX were observed in the basal region of the developing cortical wall (Figure 5C), corresponding to an early cortical plate. TBR2 positive BPs (presumably mostly basal intermediate progenitors) were concentrated in a zone between the PAX6+ progenitors and the DCX+ neurons, corresponding to the sub ventricular zone (SVZ) (Figure 5D).

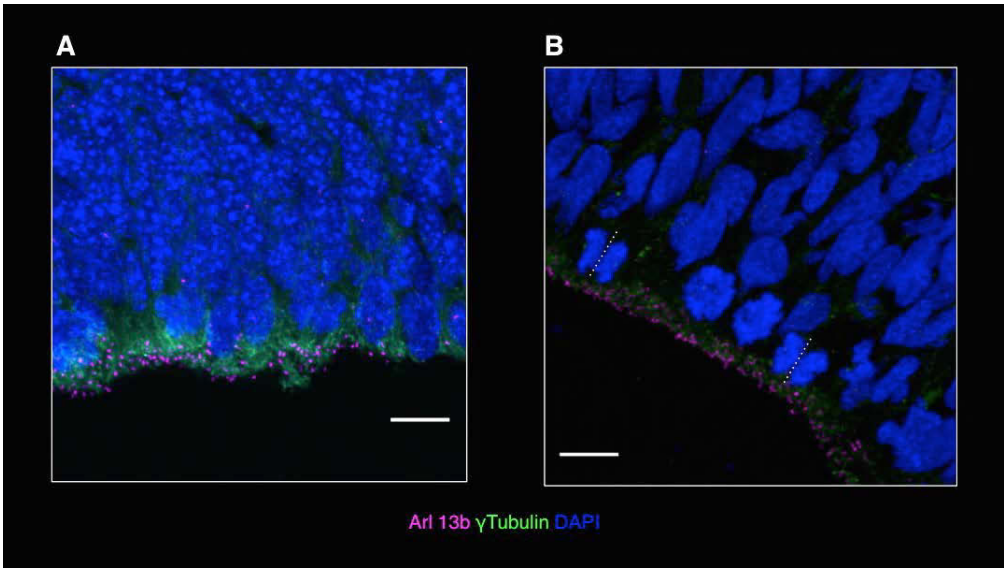

Figure 6. Features at the cortical apical boundary:

(A) Apical boundary of an E 14.5 mouse neocortex lining the ventricle showing cilia stained with Arl 13b (magenta), centrosomes stained with γ tubulin (green), and DAPI (blue).

(B) Apical boundary of a 40 days old human cerebral organoid dorsal cortex lining the ventricle showing cilia stained with Arl 13b (magenta), centrosomes stained with γ tubulin (green), and DAPI (blue). White dotted lines mark vertical cleavage plane perpendicular to the ventricle. (Scale bars, 100 μm).

Further analysis was carried out to study the cell biological characteristics of the apical progenitors. This revealed that the angle of cell division of the AP was mostly perpendicular to the apical surface lining the ventricle (Figure 6B) (Smart, 1972a; Smart, 1972b; Smart, 1973; Landrieu and Goffinet, 1979; Huttner and Brand, 1997; Estivill-Torrus et al., 2002; Kosodo et al., 2004; Fish et al., 2006; Stricker et al., 2006; Konno et al., 2008; Hansen et al., 2010; Lui et al., 2011; La Monica et al., 2013), the location of cilia was found to be apical, as well as basolateral (Figure 6B) (Cohen and Meininger, 1987; Farkas and Huttner,

2008; Wilsch-Bräuninger et al., 2012), the golgi were found to be perinuclear. Time-lapse live imaging of apical mitoses carried out during an independent study, showed apically directed nuclear migration prior to, and basally directed nuclear migration after, mitosis, consistent with the existence of interkinetic nuclear migration (Mora-Bermúdez, Badsha et al., 2016). These results suggest that human cerebral organoids recapitulate aspects of human foetal brain development and may thus allow comparisons with cerebral cortex development in human cerebral organoids and foetal neocortex.

2.2.2. Transcriptome analysis- Gene expression in human foetal cortex vs human cerebral organoid cortex:

All single cell RNA sequencing (scRNAseq) experiments were carried out by our collaborators at MPI-EVA (Dr. Barbara Treutlein and group), hence only a limited account of the scRNAseq validation is mentioned here. The full detailed validation of their work has been published (Camp, Badsha et al., 2015).

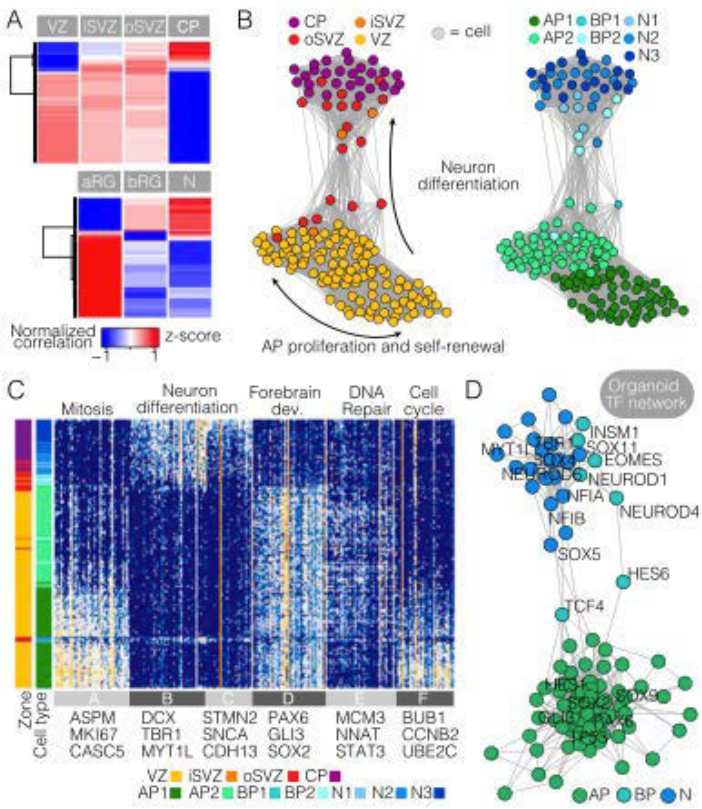

Figure 7. Data showing similar gene expression profiles characterize lineage progression in organoid and foetal cerebral cortex (Modified from Camp, Badsha et al., 2015)**:**

(A) Organoid cerebral cortex-like cells have differential correlation with bulk RNA-seq data from different laser-microdissected zones or FACS-purified cell types from foetal cerebral cortex.

(B) Organoid cell lineage network based on pairwise correlations between cells. Cells are colored based on maximum correlation to cortical zones (Left) or cell type (Right).

(C) Pseudotemporal cell ordering along the organoid lineage reveals gene expression changes from NPC to neuron. Genes with highest correlation and anticorrelation to PC1–3 are shown. Rows represent cells and columns genes. Maximum correlation to cortical zone and cell type is shown in the left sidebars.

Top GO enrichments are shown above the heat map, with representative genes listed below.

(D) Correlation network using the same TFs as in the foetal TF network reveals two highly connected subnetworks controlling AP proliferation/self-renewal and neuron differentiation. Shown are nodes (TFs) with more than two edges, with each edge reflecting a correlation between connected TFs that is greater than 0.3.

The cerebral organoids from a batch were first tested (in house) using immunofluorescence to confirm existence of dorsal cortical regions and then transported to MPI-EVA, along a one and a half hour journey, in a well-insulated box. All organoids were immediately shifted to a 37 °C incubator upon arrival and given fresh media shortly thereafter. They were allowed to remain in the incubator for a couple of days before their dissection, dissociation and subsequent scRNAseq.

Comparison of cell composition and lineage relationships in foetal and organoid cerebral cortex using scRNA-seq showed that organoid cells use similar sets of genes as their foetal counter parts to perform cortical processes such as NPC proliferation and self-renewal, production of ECM, migration, adherence, de-lamination, and differentiation that results in structured cerebral tissue (Figure 7) (Camp, Badsha et al., 2015). The gene expression profile for the production of ECM was an especially interesting finding using scRNAseq, and was confirmed using immunofluorescence to the COLV protein (Figure 8). These findings

confirmed the validation of cerebral organoids as a suitable model system to study neocortical development.

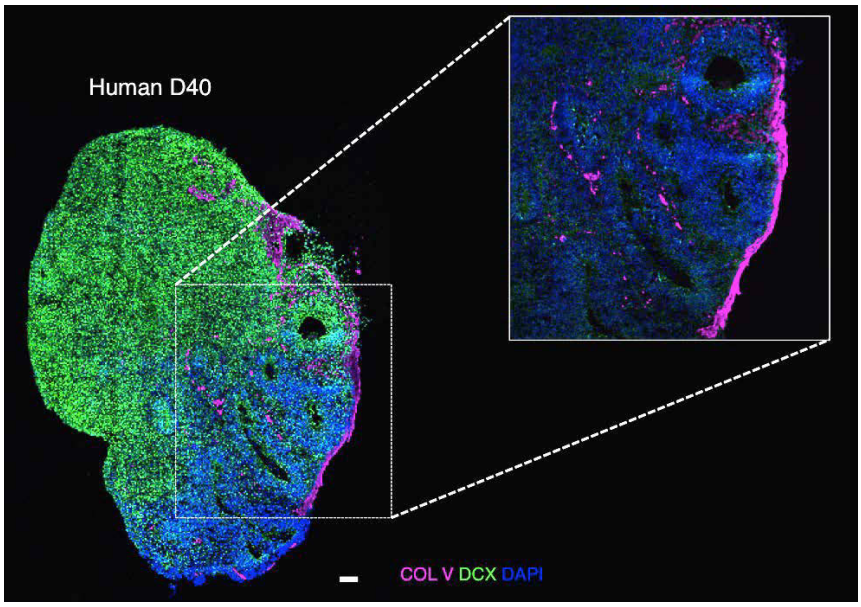

Figure 8. Extracellular matrix lining cortical regions: A 40 days old human cerebral organoid showing Collagen V expression (magenta) basal to the neurons (DCX, green) in each cortical region (DAPI, blue). (Scale bar, 100 μm).

2.3. CHARACTERIZATION OF CHIMPANZEE AND ORANGUTAN CEREBRAL ORGANOIDS BASED ON MARKER EXPRESSION:

The markers that were used to characterize the human cerebral organoids were also used to characterize the chimpanzee and orangutan cerebral organoids. Cerebral organoids were generated from induced pluripotent stem cells (iPSCs) derived from chimpanzee and orangutan fibroblasts and lymphocytes (Mora-Bermúdez, Badsha et al., 2016). The chimpanzee cerebral organoids formed complex tissue structures that resembled the developing primate brain, as reported previously for human cerebral organoids (Lancaster et al., 2013). The

cortical region of the orangutan cerebral organoids showed a temporally similar marker expression as that observed in the human organoids, although their structure was not as sophisticated as that observed in the human and chimpanzee cerebral organoids- the structure being more similar to a rosette than an organoid. Furthermore, the orangutan cerebral organoids could only be grown with a protocol slightly different from the one used to grow the human and chimpanzee cerebral organoids (discussed in the "Tried and Tested" section at the end of the dissertation). Apart from these issues, the orangutan cerebral organoids were extremely small in size and showed almost no TBR2 positivity at D30 (considered to be an early neurogenic time point), albeit showing neurons stained with DCX (Figure 9). Hence only the chimpanzee cerebral organoids were used for further analysis and comparisons.

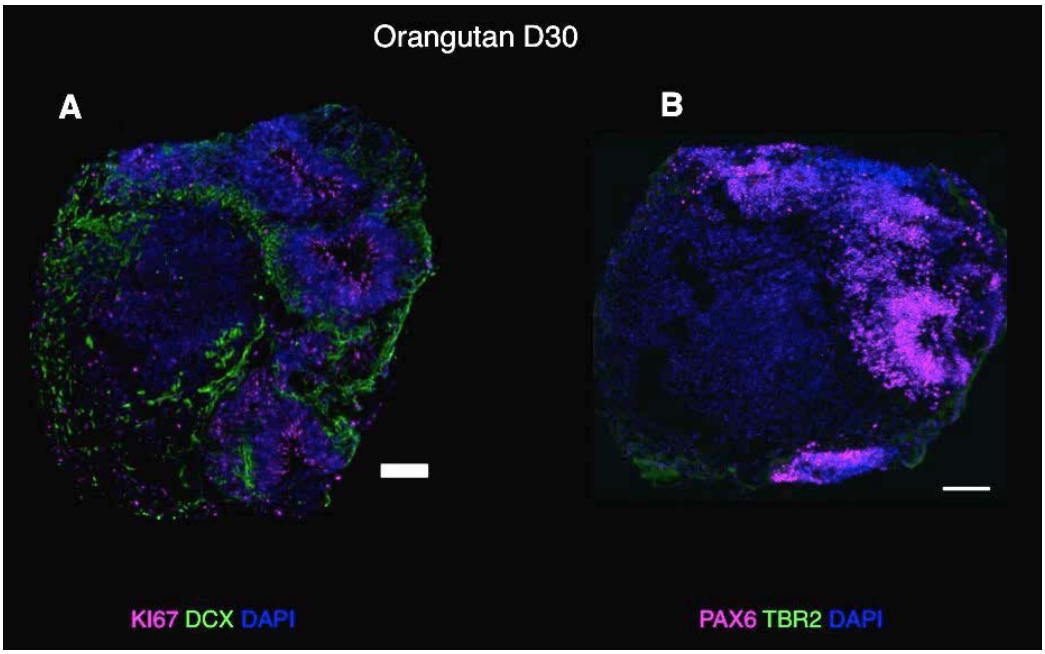

Figure 9. Orangutan cerebral organoids:

(A) A 30 days old orangutan cerebral organoid showing KI67 positive neural stem cells (magenta) and DCX positive neurons (green), and DAPI (blue). (Scale bar, 100 μm).

(B) A 30 days old orangutan cerebral organoid showing only PAX6 positivity (magenta) and an absence of TBR2 positivity, and DAPI (blue). (Scale bar, 100 μm).

2.3.1. Comparison of the progression of neurogenesis in chimpanzee cerebral organoid to that observed in the human cerebral organoid:

Similar to human iPSC-derived cerebral organoids (Camp, Badsha et al., 2015), the chimpanzee organoids grown for 52 days (D52), also showed cortex-like regions with PAX6 positive APs residing predominantly in the apical-most zone facing a ventricular lumen (Figure 10A left; Figure 10B left), similar to the ventricular zone (VZ) of developing primate neocortex at an early-mid stage of neurogenesis. Consistent with this, cells immunoreactive for the deep-layer neuron marker CTIP2 were observed in the basal region of the developing cortical wall (Figure 10A left), corresponding to an early cortical plate. TBR2 positive BPs were concentrated in a zone between the PAX6+ progenitors and the CTIP2+ neurons, corresponding to the sub- ventricular zone (SVZ) (Figure 10B left). Time-lapse live imaging of apical mitoses carried out during the same independent study as before, showed apically directed nuclear migration prior to, and basally directed nuclear migration after, mitosis, consistent with the existence of interkinetic nuclear migration (Mora-Bermúdez, Badsha et al., 2016). These results suggest that chimpanzee cerebral organoids recapitulate aspects of foetal chimpanzee brain development and may thus allow

comparisons with cerebral cortex development in human cerebral organoids and foetal neocortex.

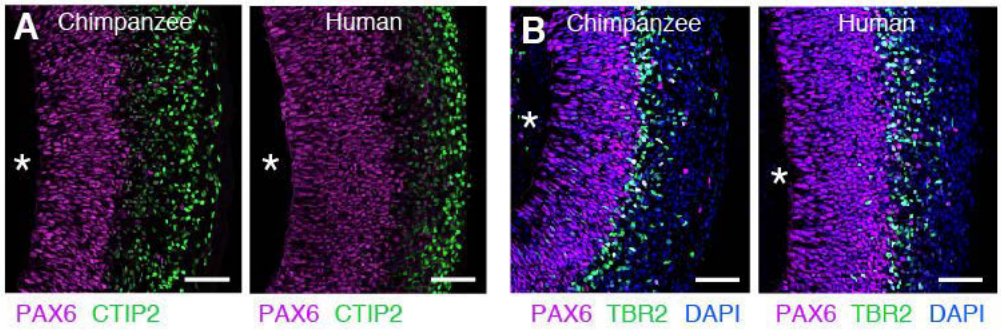

Figure 10. Comparison between human and chimpanzee cerebral organoid marker expression (Modified from Mora-Bermúdez, Badsha et al., 2016)**:**

(A) Cryosections of cortical regions from chimpanzee and human cerebral organoids at day 52 immunostained for PAX6 (magenta), CTIP2 (green), and DAPI (blue). (Asterisks, ventricular lumen; Scale bars, 50 μm).

(B) Cryosections of cortical regions from chimpanzee and human cerebral organoids at day 52 immunostained for PAX6 (magenta), TBR2 (green), and DAPI (blue). (Asterisks, ventricular lumen; Scale bars, 50 μm).

2.3.2. Transcriptome analysis- Gene expression in chimpanzee cerebral organoid cortex:

All single cell RNA sequencing (scRNAseq) experiments were carried out by our collaborators at MPI-EVA (Dr. Barbara Treutlein and group), an in depth analysis of their scRNAseq work has been published (Mora-Bermúdez, Badsha et al., 2016). About 344 single cell transcriptomes from 7 organoids ranging from 45 to 80 days were generated and combined for analysis.

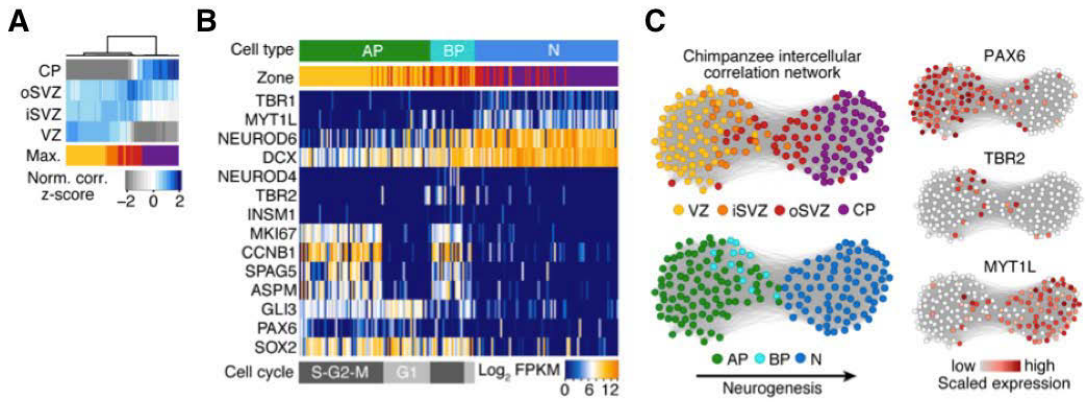

Figure 11. Chimpanzee cerebral organoids recapitulate cortex development (Modified from Mora-Bermúdez, Badsha et al., 2016)**:**

(A) Heatmap showing normalized correlation (Z-score) of single-cell transcriptomes from chimpanzee cerebral organoid cortex with bulk RNA-seq data from laser-microdissected zones (Fietz et al., 2012) from 13 wpc human neocortex.

(B) Heatmap showing expression of AP, BP, and neuron (N) marker genes. Each column represents a single cell, each row a gene. Cell type and maximum correlation to bulk RNA-seq data from cortical zones are shown in the top sidebar. APs and BPs were sub-classified based on G1-S (light grey) or G2-M (dark grey) phases of the cell cycle.

(C) Lineage network based on pairwise correlations between chimpanzee cerebral organoid cortical cells reveals a structured topology where VZ-APs connect to cortical plate (CP) neurons (N) through SVZ-BPs. Cells are coloured based on cortical zone (top left) or cell type assignment (bottom left). APs, BPs, and neurons were classified based on maximum correlation with single-cell transcriptomes from the human foetal neocortex. Expression of markers PAX6, TBR2, and MYT1L are shown to the right.

Upon comparison with bulk RNA seq data from human foetal cortical cells (Fietz et al., 2012), the analysis revealed a VZ sub-network of human and chimpanzees APs that linked through BPs expressing iSVZ and oSVZ markers to cortical plate neurons. APs, BPs, and neurons from human and chimpanzee generally intermixed, confirming that cells in the chimpanzee organoid cortices have a zonal organization consistent with what is observed histologically. The major proportion of the variation in the data was not between in vitro and in vivo tissues or between species, but among cell states during neurogenesis, confirming that the major features of the genetic programs regulating the NSPC-to-neuron lineage are conserved between human and chimpanzees, and are recapitulated in cerebral organoids from both species (Figure 11).

2.4. COMPARISON BETWEEN DEVELOPMENT OF HUMAN AND CHIMPANZEE CEREBRAL ORGANOIDS:

Previous computational studies have predicted that the increased neuron numbers in humans (~19 billion neurons) compared to chimpanzees (~6 billion neurons) in spite of very similar gestation periods (humans- 280 days, chimpanzees- 243 days), is probably ascribed to an extended neurogenic period in humans compared to chimpanzees (Lewitus et al., 2014).

Since the length of the neurogenic period of a developing cortex can be calculated in vitro using cerebral organoids, this study was carried out by comparing iPSC derived chimpanzee cerebral organoids (from two chimpanzee iPSC lines Sandra A and PR818-5) and iPSC derived cerebral organoids from two human lines (SC102A1 and 409B2). iPSC lines were used instead of ES cell lines

due to the unavailability of chimpanzee derived ES cell lines at the time of the study.

Organoids from the two species were grown simultaneously, under similar conditions, and the time of their neural induction (post germ layer differentiation) was taken as the start of neurogenesis, hence all conditions including the time frame for media change were maintained between the two species from this point on. The purpose of this study design was to observe and compare the development of the cerebral organoids from the two species at specific time points. The cerebral organoids were fixed and stained at different time points in order to study their progression over time.

2.4.1. Comparison of progression of neurogenesis between the dorsal cortices of human cerebral organoids and chimpanzee cerebral organoids:

The cortical development appeared to be remarkably similar between both human and chimpanzee cerebral organoids at the earlier stages of development (~D30) but the differences in their development became apparent around D52 when the chimpanzee organoids showed GFAP+CTIP2– cells in the cortical plate while the human cerebral organoids did not display such advancement (Figure 12). It is to be noted that neither the human nor the chimpanzee organoids at this stage had yet begun producing the late born SATB2 positive neurons. This suggested that the chimpanzee cerebral organoids could be considered to be in mid to late neurogenesis while the human organoids appeared to still be in mid neurogenesis.

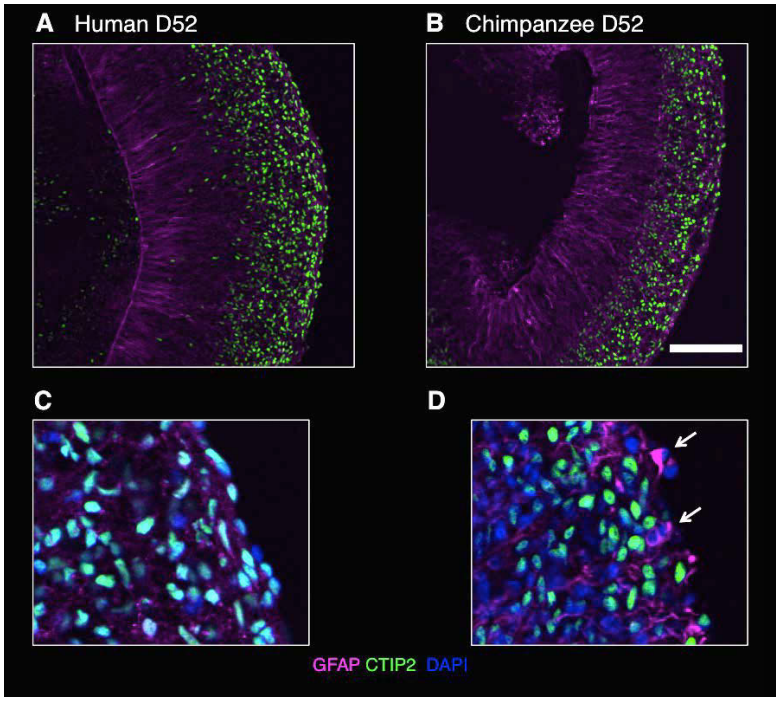

Figure 12. Earlier onset of gliogenesis in chimpanzee organoids:

(A) Cortical region from a 52 days old human cerebral organoid stained for GFAP (magenta) and CTIP2 (green).

(B) Cortical region from a 52 days old chimpanzee cerebral organoid stained for GFAP (magenta) and CTIP2 (green). (Scale bar, 100 μm).

(C) Magnified region of a human cerebral organoid cortex showing lack of GFAP+CTIP2– cells in the cortical plate.

(D) Magnified region of a chimpanzee cerebral organoid cortex showing GFAP+CTIP2– cells (marked by white arrows) in the cortical plate.

At later stages of development (~D69- 79), the dorsal cortices of the chimpanzee cerebral organoids showed an earlier onset of S100β (a late marker for oligodendrocytes and certain types of astrocytes), compared to the human cerebral organoids, which showed S100β expression in areas other than the dorsal cortical regions (Figure 13). The cortical regions of both species were

checked for the expression of PAX6, TBR2, CTIP2 and SATB2 before being considered for comparison.

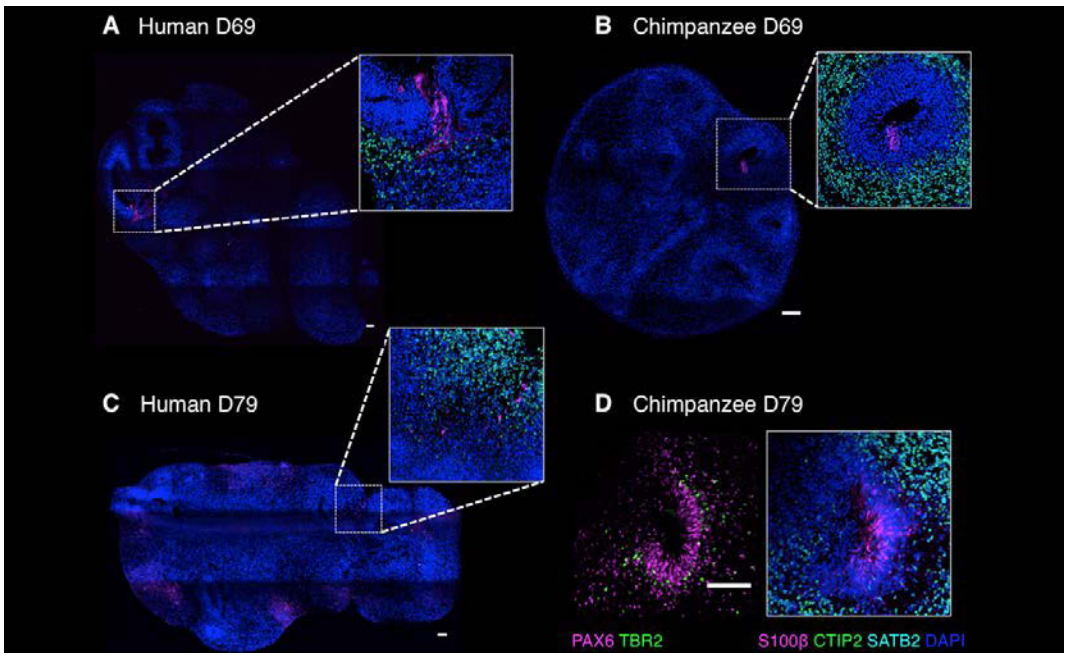

Figure 13. Later stages of neurogenesis showing S100β glial marker expression:

(A) Human cerebral organoid at D69 showing expression of S100β (magenta) in an area outside of a cortical region. Inset showing zoomed-in region of the area marked by the white box stained with S100β (magenta), CTIP2 (green), SATB2 (cyan) and DAPI (blue). (Scale bar, 100 μm).

(B) Chimpanzee cerebral organoid at D69 showing initial expression of S100β (magenta) within a cortical region. Inset showing zoomed-in region of the area marked by the white box stained with S100β (magenta), CTIP2 (green), SATB2 (cyan) and DAPI (blue). (Scale bar, 100 μm).

(C) Human cerebral organoid at D79 showing expression of S100β (magenta) in an area between two cortical regions. Inset showing zoomed-in region of the area marked by the white box stained with S100β (magenta), CTIP2 (green), SATB2 (cyan) and DAPI (blue). (Scale bar, 100 μm).

(D) Chimpanzee cerebral organoid cortex at D79 showing full blown expression of S100β (magenta) within a cortical region also stained with CTIP2 (green), SATB2 (cyan) and DAPI (blue) (right), and the same region on a different cryosection stained for PAX6 (magenta) and TBR2 (green) (left). (Scale bar, 10 μm).

Eventually the dorsal cortices of the human cerebral organoids also showed an onset of S100β (~D116) (Figure 14). Unfortunately, all three human organoids selected for analysis on D100 were of poor quality (as determined by immunostaining) and hence, the D116 human organoids were used instead for analysis.

With the progression of age, the number of identifiable cortical regions within a cerebral organoid appeared to diminish in both species, this could be a combined effect of long term culturing and neurogenic progression over time. The chimpanzee cerebral organoids appeared to show a faster depletion of CTIP2+ cortical areas than human organoids, probably owing to their faster advancement toward the end of neurogenesis and an advancing gliogenic phase (Figure 14).

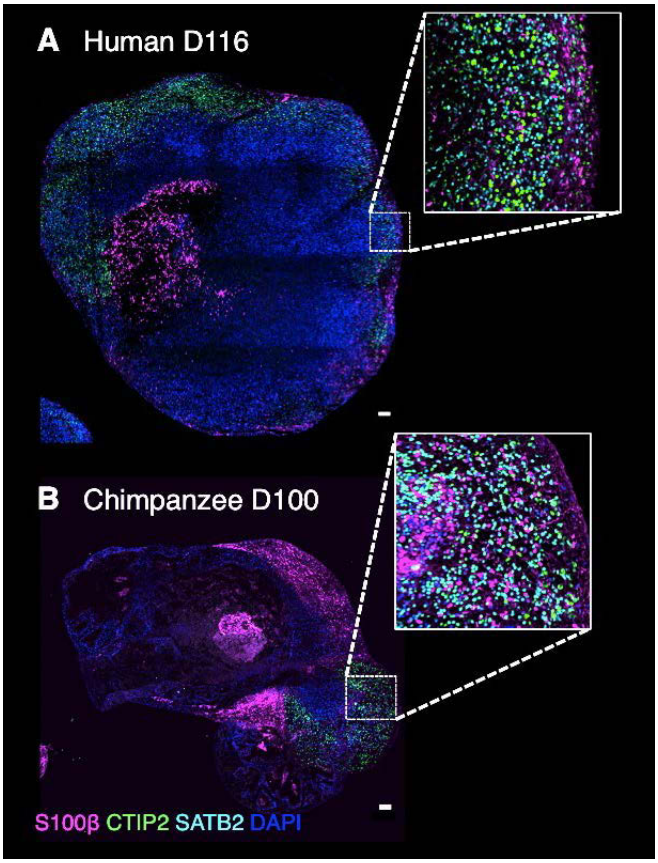

Figure 14. Gliogenesis in human cerebral organoid cortices:

(A) Human cerebral organoid at D116 showing expression of S100β (magenta) within a cortical region. Inset showing zoomed-in region of the area marked by the white box stained with S100β (magenta), CTIP2 (green), SATB2 (cyan) and DAPI (blue). (Scale bar, 100 μm).

(B) Chimpanzee cerebral organoid at D100 showing expression of S100β (magenta) within a cortical region. Inset showing zoomed-in region of the area marked by the white box stained with S100β (magenta), CTIP2 (green), SATB2 (cyan) and DAPI (blue). (Scale bar, 100 μm).

2.5. FACTORS INFLUENCING LONGER NEUROGENIC PERIOD IN HUMAN CEREBRAL ORGANOID CORTICES COMPARED TO CHIMPANZEE ORGANOID CORTICES:

The longer neurogenic period of the human cerebral organoids could be attributed to a number of factors ranging from cell cycle features of a specific cell type to the cell type composition of the whole cell population during development. It has been shown previously that features like a shorter cell cycle length or a longer S- phase length are indicative of a more proliferative state of a progenitor cell type (Betizeau et al., 2013; Arai et al., 2011) and that a higher population of proliferative progenitors is indicative of a higher neuronal output (Rakic, 1995; Lui et al., 2011; Borrell et al., 2012; Borrell et al., 2014). In order to test if this indeed was the case in this study, an analysis of the differences in the cell cycle lengths between human and chimpanzee cortical progenitors was carried out, along with an assessment of the population of the different cell types.

2.5.1 Analysis of the proliferative capacity of human and chimpanzee cortical progenitors:

In order to ascertain whether the observed advanced development in the chimpanzee organoids was simply due to a more differentiated state of the progenitors, their proliferative state and their ability to re-enter cell cycle were investigated. The proliferative state of the cortical progenitors could be ascertained by the total number of KI67 positive cells in a given area of the cortical wall of the cerebral organoids, while the ability to re- enter cell cycle

could be determined by using a combination of KI67 staining and EdU incorporation.

2.5.1.1. Estimation of the total number of proliferating cortical progenitors between human and chimpanzee cerebral organoids:

There appeared to be no significant difference in the total number of proliferating cortical progenitors between human and chimpanzee cerebral organoids as observed with KI67 staining (Figure 15). In order to re-confirm this data, this staining was carried out with two different sources of the KI67 antibody. Both yielded similar results.

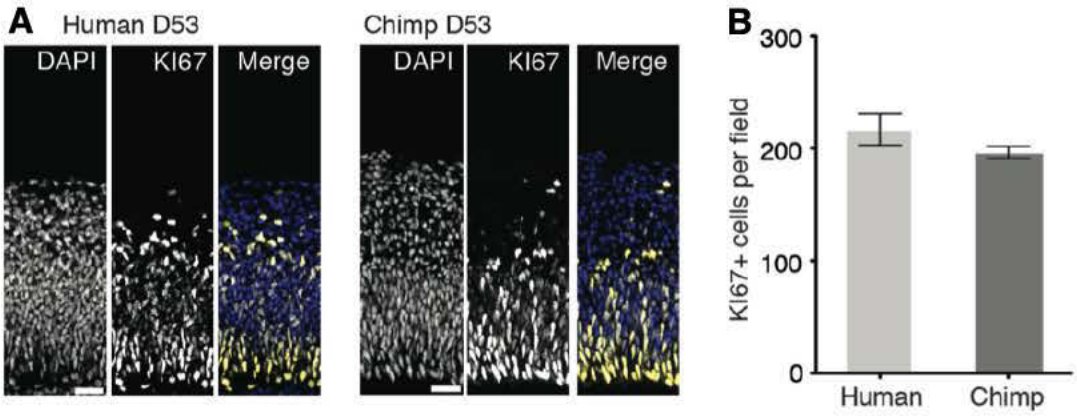

Figure 15. Comparison of proliferative progenitors between human and chimpanzee cerebral organoid cortices (Modified from Mora-Bermúdez, Badsha et al., 2016)**:**

(A) Cryosections of cortical regions from human and chimpanzee organoids at D53 immunostained for KI67 (yellow) combined with DAPI staining (blue). (Scale bars, 20 μm).

(B) Quantification of KI67+ cells in a 100 μm wide field in human and chimpanzee organoids at D52-D53 (n=7). Error bars, SEM.

2.5.1.2. Estimation of the number of actively cycling cortical progenitors between human and chimpanzee cerebral organoids:

In order to determine whether the cortical progenitors of the chimpanzee cerebral organoids simply exhibited a more restricted neurogenic state than those of the human cerebral organoids, a pulse- chase EdU experiment was carried out on 51 days old human and chimpanzee cerebral organoids.

EdU gets incorporated into the cells during the S-phase of their cell cycle and remains in the cell until it gets diluted out due to repeated rounds of cell division. A one-hour pulse of EdU was given to 51 days old cerebral organoids followed by a 24- hour chase. The cerebral organoids were then fixed and stained with KI67 followed by EdU detection (for full details, please refer the materials and methods section).

The cells that showed positivity for both KI67 proliferation marker (which marks all phases of the cell cycle except the G0 phase) and EdU were considered to be actively cycling cells whereas those that were negative for KI67 but were positive for EdU were thought to have exited the cell cycle.

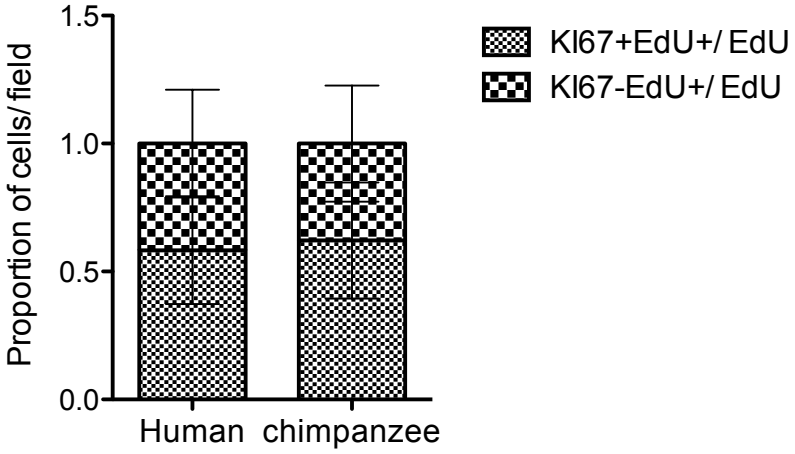

Figure 16. Estimation of cell cycle re-entry of organoid cortical progenitors: Quantification of KI67 positive and negative cells over total EdU+ cells in a 100 μm wide field in human and chimpanzee organoids at D52 (n=3). Error bars, SD.

There was no significant difference in the total proportion of KI67+EdU+ cells between human and chimpanzee cerebral organoids after 24 hours (Figure 16). This experiment was conducted under the assumption that within 24 hours after the S-phase labeling, the labeled cortical progenitor would have undergone mitosis yielding daughter cells that may or may not re-enter the cell cycle. In order to have more accurate results, the total cell cycle lengths of the human and chimpanzee cortical progenitors were calculated.

2.5.2. Cell cycle lengths analysis and their differences between human and chimpanzee cortical progenitors:

Since the cell cycle length of neural progenitors is related to their proliferative and neurogenic potential (Dehay and Kennedy, 2007; Salomoni and Calegari, 2010), the cell cycle lengths of the different cortical cell types were calculated. In

order to calculate the cell cycle length of the cortical progenitors of the human and chimpanzee cerebral organoids, the growth of the organoids from both species was staged in the same way as was done during the initial comparison of the organoids (mentioned above). Since ~D50 showed differences between mid and late neurogenesis between the two species, EdU was added to 52 days old cerebral organoids at a final concentration of 1 µg/ml (added from a 1 mg/ml EdU stock in PBS). The organoids were supplied with fresh medium containing EdU every six hours for up to 48 hours. Organoids were then collected in triplicates at the indicated time points (1, 2, 6, 24, 30/36, 48 hours) and processed as described in the materials and methods section below. The data thus acquired was processed and the cell cycle lengths of the different cortical progenitors were calculated using simple regression based on the Nowakowski method (Nowakowski et al., 1989).

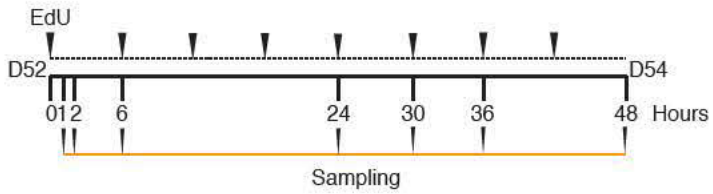

Figure 17. Schematic representation of the cumulative EdU labeling experiment (Modified from Mora-Bermúdez, Badsha et al., 2016).

2.5.2.1. Cell cycle length of apical progenitors (PAX6+TBR2– cells):

There appeared to be no significant difference in the total cell cycle length between the more neural stem cell like human (46.5 hours) and chimpanzee PAX6+TBR2– (43.8 hours) progenitors except for a longer S- phase in human progenitor cells compared to the chimpanzee which suggests a greater

proliferation potential in human cells compared to chimpanzee (Figure 18) (Arai et al., 2011). This data corroborates recently published data on cell cycle length of PAX6+ progenitors in human and chimpanzee rosettes by Otani et al., 2016.

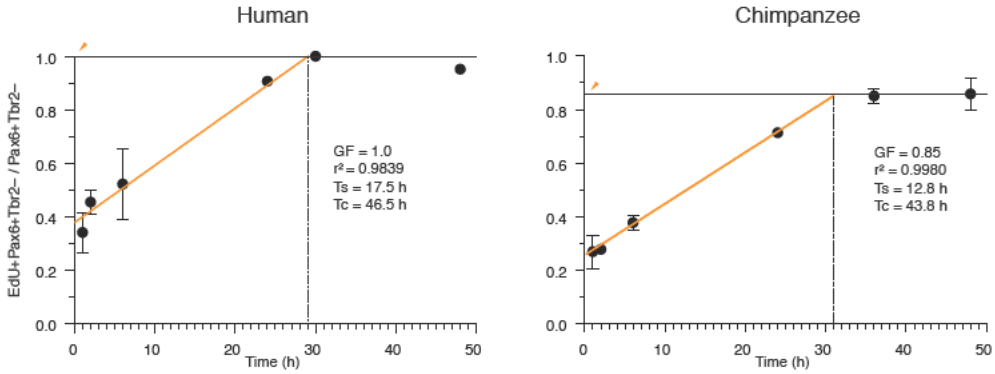

Figure 18. Determination of cell cycle parameters of human and chimpanzee organoid APs (PAX6+TBR2–) using cumulative EdU labeling (Modified from Mora-Bermúdez, Badsha et al., 2016)**:** The total cell cycle length (Tc), S- phase length (Ts), co-efficient of determination (r2) and growth fraction (GF) for human (left) and chimpanzee PAX6+TBR2– cortical progenitors. Orange arrow indicates growth fraction (n = 3 per time point). Error bars, SD.

2.5.2.2. Cell cycle length of basal progenitors (PAX6+TBR2+ cells):

The total cell cycle length of the PAX6+TBR2+ progenitor cells was also similar between both species with a longer S- phase in human cells compared to chimpanzee cells (Figure 19) suggesting higher proliferative potential in human cells than chimpanzee cells.

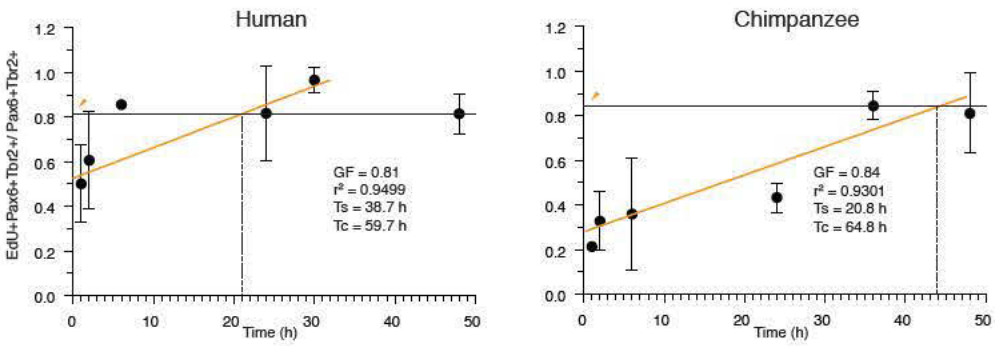

Figure 19. Determination of cell cycle parameters of human and chimpanzee organoid BPs (PAX6+TBR2+) using cumulative EdU labeling: The total cell cycle length (Tc), S- phase length (Ts), co-efficient of determination (r2) and growth fraction (GF) for human (left) and chimpanzee PAX6+TBR2+ cortical progenitors. Orange arrow indicates growth fraction (n = 3 per time point). Error bars, SD.

2.5.2.3. Cell cycle length of basal progenitors (PAX6–TBR2+ cells):

The more neurogenic PAX6–TBR2+ progenitor cells were relatively low in number and the data thus obtained from their analyses may not be best representative of the actual scenario. The total cell cycle length and the S- phase were relatively longer (~ 9 hours longer) in the chimpanzee cortical progenitors than in the human (Figure 20).

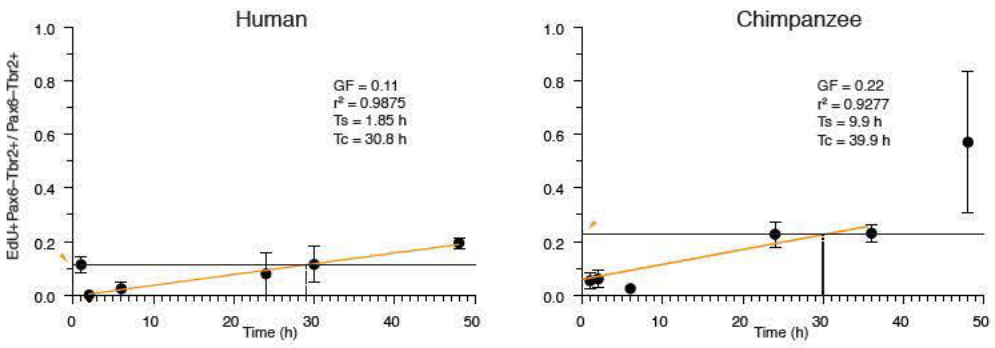

Figure 20. Determination of cell cycle parameters of human and chimpanzee organoid BPs (PAX6–TBR2+) using cumulative EdU labeling: The total cell cycle length (Tc), S- phase length (Ts), co-efficient of determination (r2) and growth fraction (GF) for human (left) and chimpanzee PAX6–TBR2+ cortical progenitors. Orange arrow indicates growth fraction (n = 3 per time point). Error bars, SD.

2.5.3. Comparison between human and chimpanzee organoid cell composition:

In order to examine the early maturation of the chimpanzee organoids in comparison to the human cerebral organoids, a comparison of the proportion of various NSPC types (as revealed by expression of PAX6 and/or TBR2) and neurons at D28 and D52-D54 between human and chimpanzee cerebral organoid cortices (Figure 21) was carried out. In both species, a decrease in PAX6+TBR2–, apically located NSPCs (presumably proliferating APs) from D28 to D52, concomitant with an increase in PAX6+TBR2+ and PAX6–TBR2+, basally located progenitor cells (presumably neurogenic BPs) (Figure 21A, B) was observed. No significant differences were observed at D28, however, at D52-D54, the proportion of PAX6+TBR2+ progenitor cells in the chimpanzee organoids was nearly twice as that in the human organoids, and the proportion

of PAX6+TBR2– NSPCs was correspondingly lower, with a significant decrease in chimpanzee PAX6+TBR2– NSPCs compared to the human PAX+TBR2– NSPCs (Figure 21B).

It was also observed that, albeit given only a small proportion, there were almost twice as many PAX6+TBR2+ progenitor cells within the VZ (~29% of total PAX6+TBR2+ progenitor cells) in chimpanzee organoids than in the VZ of human organoids (~12% of total PAX6+TBR2+ progenitor cells) (Figure 22). The area below a 3 cell gap from the outer most PAX6+ pseudostratification border was considered as "VZ" for this quantification due to the uneven borders of pseudostratification observed in some organoids. No significant difference between human and chimpanzee was observed for PAX6–TBR2+ progenitor cells (Figure 21B).

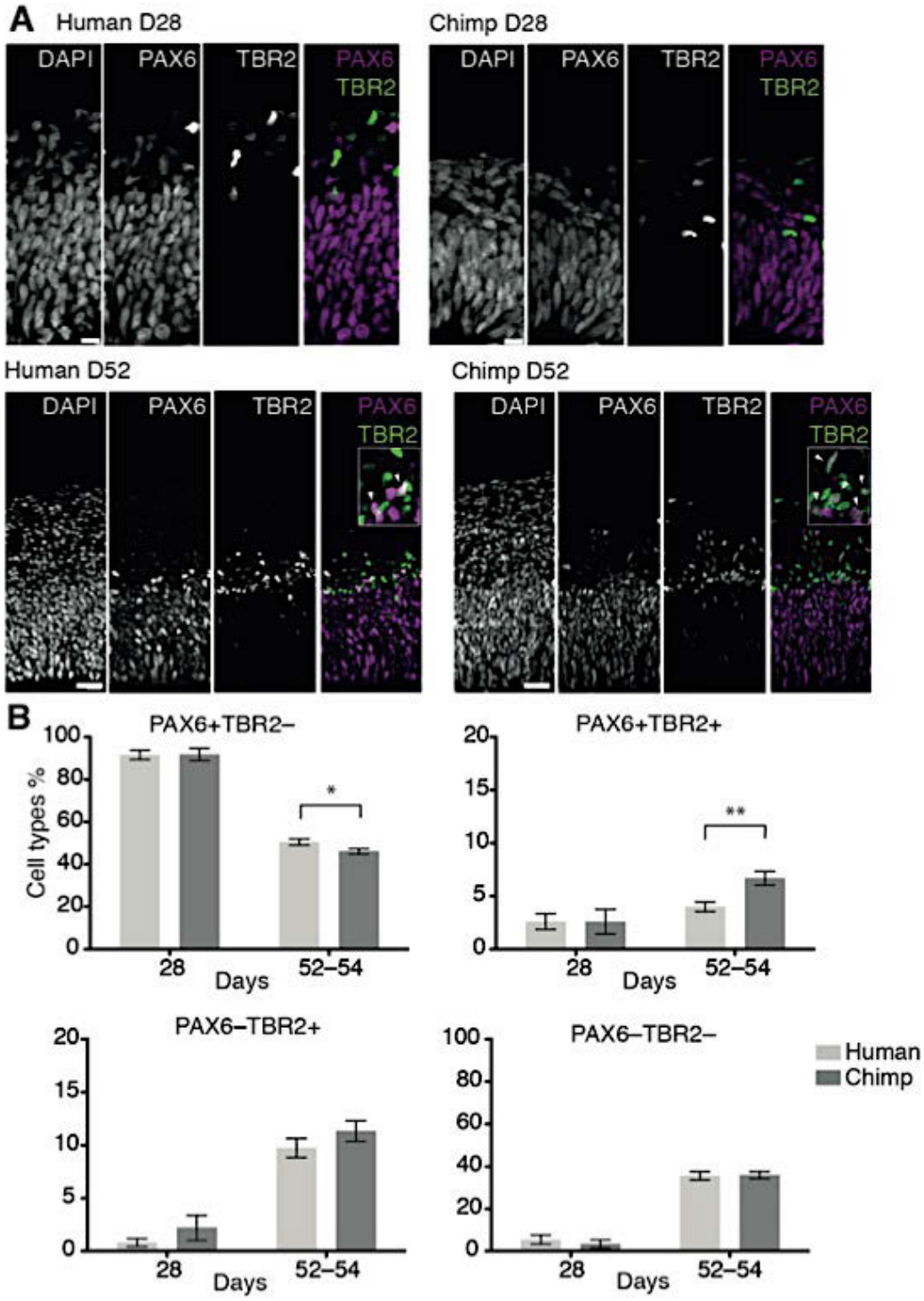

Figure 21. Changes in the proportion of cortical NSPC subtypes and neurons during human and chimpanzee cerebral organoid development (Modified from Mora-Bermúdez, Badsha et al., 2016)**:**

(A) Cryosections of cortical regions from human and chimpanzee organoids at day 28 and day 52 immunostained for PAX6 (magenta) and TBR2 (green)

combined with DAPI staining. Scale bars; D28, 10 µm; D52, 20 µm. Insets in the D52 merge images show selected areas with PAX6+TBR2+ double-positive nuclei (arrowheads) at higher magnification.

(B) Quantification of the percentage of PAX6+TBR2–, PAX6+TBR2+, PAX6–TBR2+ and PAX6–TBR2– cortical cells in human (light grey) and chimpanzee (dark grey) organoids at D28 (n = 5 organoids, 50 µm wide field) and D52-D54 (n = 17 organoids, 100 µm wide field). Error bars, SEM; * p <0.05, ** p <0.01.

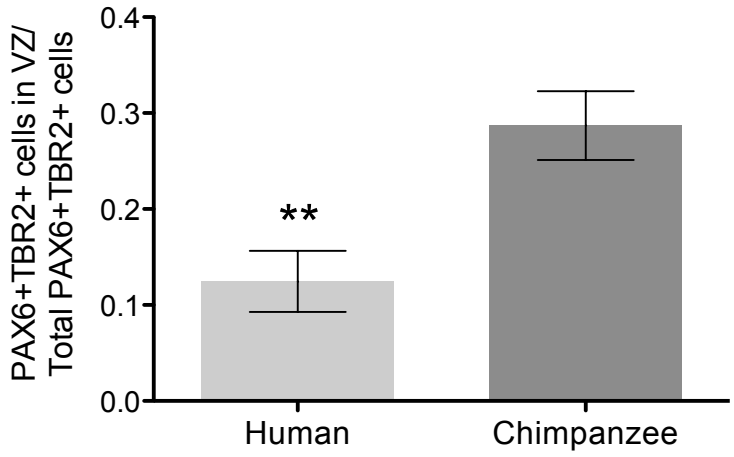

Figure 22. Quantification of PAX6+TBR2+ cells in VZ (from previous figure): Human (light grey), chimpanzee (dark grey). (n = 17 organoids, 100 µm wide field). Error bars, SEM; ** p <0.01.

In line with what would be expected with regard to neuron production, the proportion of PAX6–TBR2– cells, located in the basal-most zones of the developing cortical wall, was very low at D28 but increased by D52-D54 to about a third of the total cells for both, human and chimpanzee cerebral organoids (Figure 21B). Immunostaining for CTIP2 corroborated the neuronal identity of these cells (Figure 23).

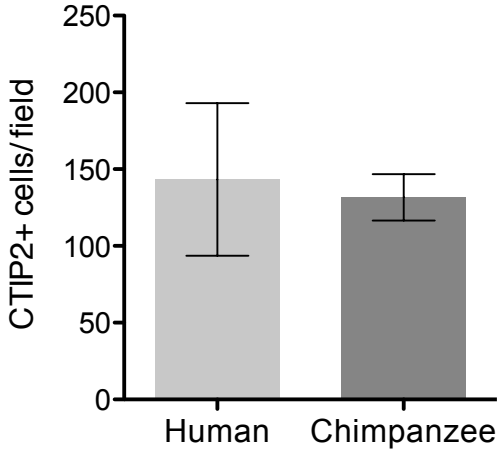

Figure 23. Quantification of cortical neuron number at D52 human and chimpanzee cerebral organoids: There is no significant difference observed in the CTIP2 positive neuron number at this stage of the cerebral organoid cortices between humans (light grey) and chimpanzees (dark grey). (n = 3 organoids, 100 μm wide field). Error bars, SD.

Considering the observation that the total proportion of NSPCs relative to neurons was virtually identical in human and chimpanzee organoids (Figure 21B) with the exception of PAX6+TBR2+ progenitor cells and their distribution, it is safe to make two conclusions here, (i) that, at the two stages studied, there are no major differences between human and chimpanzee cerebral cortex developing in organoid culture with regard to the types of NSPCs and their abundance, or neuron output, (ii) that there might be an inherent difference in the PAX6+TBR2– neural stem cell like apical progenitors between the two species, with APs from chimpanzee cortices programmed to differentiate into neurogenic progenitors faster (earlier) than the human APs.

2.5.4 Differential gene expression between human and chimpanzee cerebral organoids:

Since the single cell transcriptomes from all ages from 45 to 80 were pooled for both species before analysis, subtle differences that could have explained the faster advancement of cortical development observed at mid- late neurogenesis in chimpanzee cerebral organoids could not be singled out. However, comprehensively put, the differential gene expression analysis done by Dr. Treutlein and group, showed that about 94% of genes that were AP specific or neuron specific were not differentially expressed between humans and chimpanzees (Figure 24). Of genes specific to APs, a subset were indeed differentially expressed between the two species (APOLD1, BICC1, EFNB1, GSTM1, IFI44L, ITGB8, SDK2, SEMA5A, SLC35F1, ZNF516), these genes could be potential candidates for studying the regulation of AP proliferation in humans.

A more detailed gene expression study at specific landmark time points (such as D28, D52, or D116 etc.) could contribute to a better understanding of the progression of neurogenesis in humans and chimpanzee cerebral organoid cortices.

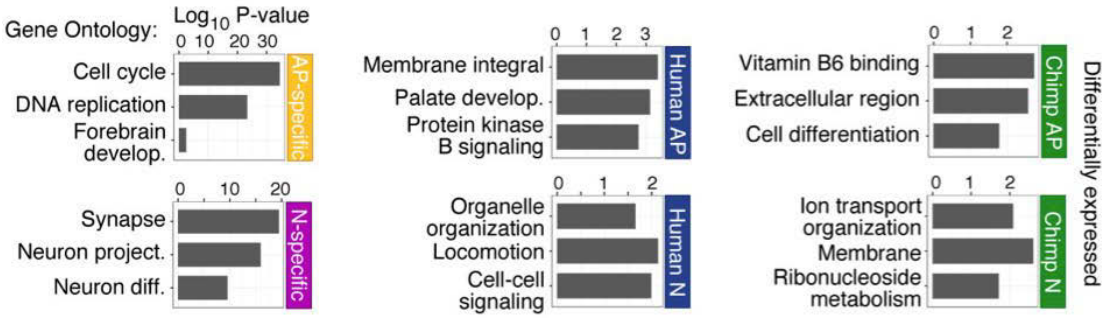

Figure 24. Gene ontology enrichments (-log10 P-value) for differentially expressed gene groups (Modified from Mora-Bermúdez, Badsha et al., 2016)**:** Left, human APs (yellow) and neurons (N, purple) that are not differential between human and chimpanzee. Center, upregulated in human APs (top) or neurons (N, bottom) compared to chimpanzee. Right, upregulated in chimpanzee APs (top) or neurons (N, bottom).

2.6. OTHER DIFFERENCES FOUND BETWEEN HUMAN AND CHIMPANZEE CEREBRAL ORGANOIDS:

Apart from differences in general progression of neurogenesis between humans and chimpanzees, another striking difference that was noticed immediately, (and in blinded experiments), is the difference in the number of mitotic cells present in the two species. Cell nuclei in the mitotic stages from prophase to anaphase were marked by PH3 and the cells in the mitotic stages from prophase to telophase were marked by pVIM. Majority of the mitosis observed was along the apical surface lining the ventricles of the cortices. There was little or no basal mitosis observed in most organoid cortices.

At D52 the human organoid cortices showed almost twice the amount of cells in mitosis than the chimpanzee cortices (Figure 25). This result could have been

attributed to the farther progression of neurogenesis in chimpanzees, given the onset of gliogenesis at this stage, except that the same result was also observed in D30 cerebral organoids in a blinded experiment.

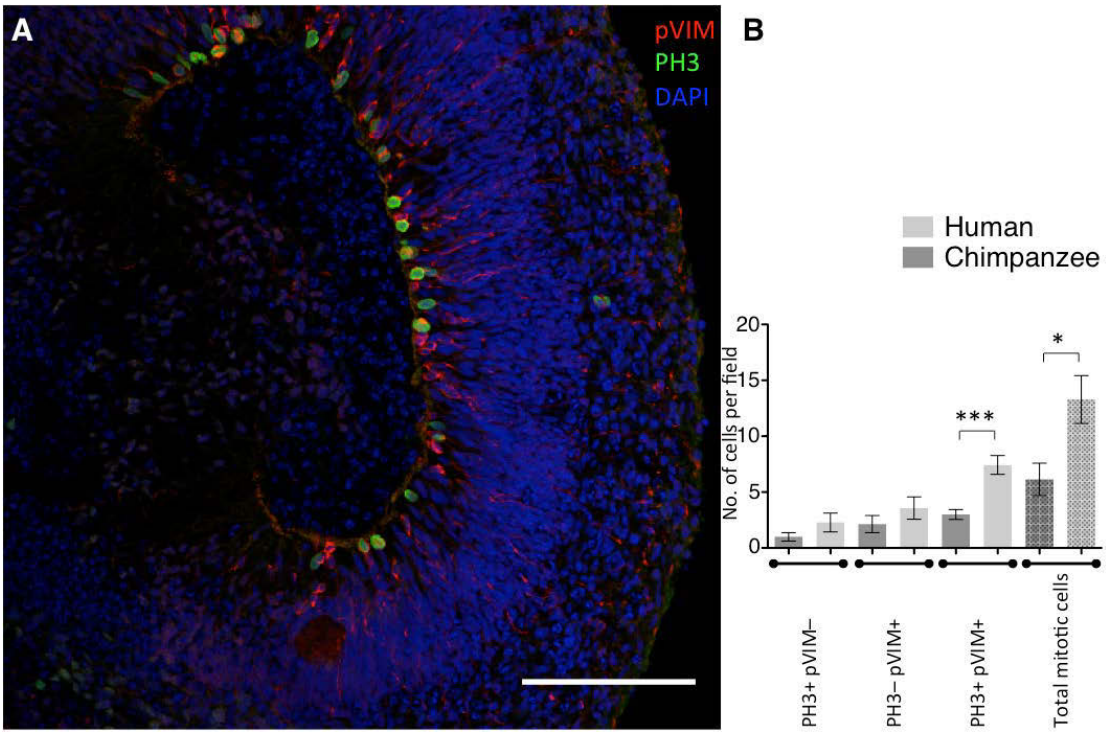

Figure 25. Differences in number of mitotic cells in human and chimpanzee cerebral organoids:

(A) Representative image of a D52 human cerebral organoid cortex showing apical and basal mitosis, marked by PH3 (green), pVIM (red) and DAPI (blue). Scale bar, 100 µm.

(B) Quantification of mitotic cells in a 100 µm wide field in human (light grey) and chimpanzee (dark grey) organoids at D52 (n=7). Patterned bars denote "total mitotic cells". Error bars, SEM. * p <0.05, *** p <0.001.

The implication or cause for this result is not yet clear. Independent live imaging studies (Mora-Bermúdez, Badsha et al., 2016) showed that there was no

significant difference in the overall mitotic length between human and chimpanzee APs, thus negating the chances of an accumulation of mitotic APs at the apical surface at any given point of time due to an extended mitotic length, in humans. However, since these studies were carried out in conditions different from the culturing conditions of the organoids such that the APs were exposed to a collagen matrix that was used for the embedding of the organoid during live imaging and kept so overnight (during a typical experiment), it remains to be seen whether these observations could be due to a difference in responsiveness to the collagen matrix used, between the human and chimpanzee APs (which are otherwise enclosed within the cortex, sheltered from any direct contact with a matrix or media). Unfortunately, the mitotic length could also not be effectively deduced from the EdU cell cycle length experiments and thus an explanation or the significance of this difference in the number of mitotic cells between humans and chimpanzees remains to be seen.

3. Discussion

3.1. CEREBRAL ORGANOIDS AS A MODEL SYSTEM:

Studying the neocortical development of primates in general has always been a challenge given the limiting ethical factors involved. The embryonic neocortical tissues acquired from aborted pregnancies could also only be grown and studied for a period as short as one or two weeks in laboratory conditions (Hansen et al., 2010; La Monica et al., 2013; Betizeau et al., 2013). Thus, it was a huge advantage for neuroscience researchers when advancements were made in 3D stem cell based bioengineering resulting in cerebral organoids (Lancaster et al., 2013; Kadoshima et al., 2013), as this enabled the study of neocortical development right from the embryonic neural induction stage up to the late stages of neurogenesis while maintaining the organoid cultures in bioreactors for periods as long as even one year (Lancaster, personal correspondence). Although it became evident from initial characterization studies that these cerebral organoids mimic in vivo neocortical development, their reproducibility and their ability to recapitulate the developmental transcriptional programs remained to be seen.

The work described in this thesis, addressed both these issues by combining immunofluorescence studies on fixed organoid tissue over the course of their development and an unbiased transcriptional analysis on organoid derived single cells, (albeit the latter was carried out by a collaborating lab).

The initial immunofluorescence characterization studies showed that the cerebral organoids grown in house faithfully produced forebrain regions, as evidenced by FOXG1 expression in their ventricle enclosing cortical “buds”.

Following this, the usage of markers for neural stem cells (PAX6) and neurogenic progenitors (TBR2) (Englund et al., 2005) indicated that the spatiotemporal expression of these markers, as seen in live tissue, was also maintained in the cortices of these cerebral organoids, with the TBR2 expression being turned on sequentially after PAX6 expression, as the progenitors lost their self- renewal capacity and became more neurogenic (Englund et al., 2005). With further progression in organoid neurogenesis, other aspects of in vivo neocortical development such as the temporal expression of early (TBR1), mid (CTIP2) and late born (SATB2) neuronal markers, the expression of ECM proteins and other aspects of cell biology such as cleavage plane orientation, INM etc., were also recapitulated (Camp, Badsha et al., 2015; Mora-Bermúdez, Badsha et al., 2016). The protocol used, however, had the limitation of not forming the six-layered cortical plate as seen in the animal tissue, this issue has been recently addressed by employing the usage of biopolymers, its reproducibility (in house) is yet to be determined (Lancaster et al., bioRxiv 2016).

Unbiased transcriptional studies using pooled single cell RNA sequencing data from unlabeled dissociated organoid cortical cells confirmed the recapitulation of in vivo transcriptional programs in cerebral organoids (Camp, Badsha et al., 2015; Mora-Bermúdez, Badsha et al., 2016). A more comprehensive transcriptome study using data from organoid cells from specific time points (as was done for the immunofluorescence studies) would be more useful in capturing the temporal progression of neurogenesis instead of a pseudotemporal ordering of events from existing pooled data.

3.2. CORTICAL CELL DIVERSITY IN CEREBRAL ORGANOIDS:

Apart from rendering an insight into the developmental progression of neurogenesis in cerebral organoids, markers such as PAX6 and TBR2 also gave an insight into the various types of progenitor cells present in the cortices of cerebral organoids. Based on the expression (or lack thereof) of these neural stem cell and neurogenic cell markers, at least three types of progenitors came to be identified.

(i) PAX6+TBR2– progenitor cells:

These cells formed the majority of the progenitor cell population with most of them localized at the ventricular zone (VZ), arranged in a pseudostratified manner and could thus be termed apical progenitors. These apical progenitors underwent INM and showed apical progenitor characteristics like the presence of an apical primary cilium, a vertical cleavage plane and a high self- renewing capacity.

(ii) PAX6+TBR2+ progenitor cells:

These cells were mainly localized in the region between the PAX6+TBR2– progenitor cells and the PAX6–TBR2– progenitor cells (considered to be the putative SVZ). It could be argued that these cells could just be progenitor cells transitioning from a neural stem cell- like state to a more neurogenic state, instead of being a whole different class of progenitors by themselves, however, previous studies in other animal models (Lui et al., 2011; Poluch and Juliano, 2013) have identified such cells in the SVZ to be the transit amplifying cells (TAPs) which could play an important role in the expansion of the neocortex.

Since the immunostaining for pVIM could only rarely outline the processes of the progenitor cells (owing to the staining technique or the antibody interaction or even the angle of cryosectioning), the polarity of these cells could not be determined.

(iii) PAX6–TBR2+ progenitor cells:

These cells were localized to the putative SVZ region of the organoid cortex and were very few in numbers. They were dispersed along with the PAX6+TBR2+ progenitor cells in this region. Given that their polarity could also not be defined owing to the reason mentioned above, their identity remains speculative at this point, with the closest identity that could be conferred upon them being that of the intermediate progenitors (IPs) (Kowalczyk et al., 2009).

(iv) PAX6–TBR2– cells:

These cells were localized above the region termed as the SVZ and were identified to be neurons using neuronal markers (e.g., CTIP2). Their full functioning capacity as neurons remains to be studied, although preliminary studies on their ability to fire have been explored (Lancaster et al., 2013).

3.3. DIFFERENCES IN CORTICAL CELL COMPOSITION BETWEEN HUMAN AND CHIMPANZEE ORGANOIDS REFLECTS A MORE NEUROGENIC FATE FOR CHIMPANZEE PAX6+TBR2– NSPCs:

There was no major difference in the composition of the cortical cells between human and chimpanzee cerebral organoids during the early stages of development (D28), however with the progression of neurogenesis, it slowly

became apparent that the progenitors of the chimpanzee organoid cortices were shifting toward a more neurogenic fate as evidenced from a decrease in the PAX6+TBR2– progenitor cells followed by an increase in the PAX6+TBR2+ progenitor cells which was twice as that of the increase observed in the human PAX6+TBR2+ progenitor cells.

Given that the numbers of PAX6–TBR2+ progenitor cells and the PAX6–TBR2– cells remained similar between the two species, while there was a slight yet significant difference in the decrease of PAX6+TBR2– progenitor cells in chimpanzee organoids compared to human organoids, along with observation that a higher percentage of the PAX6+TBR2+ progenitor cells were found in the chimpanzee VZ than the human VZ, it can be reasoned that the PAX6+TBR2– progenitor cells of the chimpanzee organoids were adopting a more neurogenic fate by turning on TBR2 expression (Englund et al., 2005). This might be a reflection of either an advanced stage of neurogenesis in the cortices of chimpanzee organoids compared to human organoids or just a lesser proliferative state of NSPCs in chimpanzees compared to humans. The latter was, however, found to not be the case considering the observation that the overall KI67+ positivity of the NSPCs appeared to be similar between both species. The proliferative capacity of individual types of progenitor cells remains to be studied (due to limitations in immunostaining).

A more detailed study with lineage tracing of the PAX6+TBR2– NSPCs would help in determining the actual fate of these progenitor cells and answer the question of whether there is an inherent difference in the apical cortical

progenitor cells between humans and chimpanzees and if this difference ultimately contributes to a bigger expansion of the neocortex in humans compared to the chimpanzees.

3.4. CELL CYCLE CHARACTERISTICS OF HUMAN AND CHIMPANZEE ORGANOID CORTICAL PROGENITORS SUGGEST A HIGHER PROLIFERATIVE CAPACITY FOR HUMAN PAX6+TBR2– NSPCs:

Cell cycle length measurements of the different progenitor cell types showed that even though there was no major difference in the overall cell cycle length between human and chimpanzee progenitor cells, the S- phase length of the human PAX6+TBR2– NSPCs (Mora-Bermúdez, Badsha et al., 2016) and the PAX6+TBR2+ progenitor cells was longer than that of the chimpanzee progenitor cells. Studies in mouse have shown that the mouse Tis21::GFP negative (proliferative) APs have a longer S-phase than Tis21::GFP positive (differentiative) APs (Arai et al., 2011). Thus the longer S-phase of human than chimpanzee APs observed here is in line with the notion that human APs having a greater tendency for proliferative divisions.

Live imaging studies done on younger organoids (D30) in an independent study (Mora-Bermúdez, Badsha et al., 2016) showed that the prometaphase-metaphase is longer in human APs than in chimpanzee APs. This difference was also observed between human and orangutan APs. Previous observations that the mouse Tis21::GFP negative APs, which are known to undergo proliferative divisions to generate more APs, have a longer prometaphase-metaphase than Tis21::GFP positive APs, which are known to undergo neurogenic divisions to

generate BPs (Haubensak et al., 2004), the longer prometaphase-metaphase in human than chimpanzee APs would therefore be consistent with a greater tendency for proliferative than neurogenic divisions.

3.5. GENE EXPRESSION STUDIES OF ORGANOID CORTICAL CELLS REFLECT INHERENT EVOLUTIONARY ADAPTATIONS:

The gene ontology enrichments for differentially expressed gene groups (Figure 24) (Mora-Bermúdez, Badsha et al., 2016) of human and chimpanzees cortical APs and neurons showed that genes for "palate development" were up regulated in human APs compared to chimpanzee APs, reflecting the evolutionary change of a wider palate seen in humans compared to chimpanzees.

Another notable gene ontology term that is of interest is the up regulation of genes for "vitamin B6 binding" and "cell differentiation" in chimpanzee APs compared to human APs. Studies in rats have shown that vitamin B6 is an important co-factor required for various neurodevelopmental processes such as differentiation of neurons, development of neuronal morphology and synaptogenesis in both neocortex and the hippocampus (Groziak SM and Kirksev A, 1987; Groziak SM and Kirksev A, 1990; Guilarte TR, 1993). Thus, a higher expression of genes required for vitamin B6 binding in chimpanzees at the time points studied, could reflect a higher propensity for neuronal differentiation in chimpanzee APs compared to human APs, this assumption is re-enforced by the up regulation of genes for "cell differentiation" in chimpanzee APs compared to human APs. Considering the fact that the APs are located deep within the cortical region, towards the ventricle and away from the organoid

surface that is exposed to media, the chances of this observation occurring due to differences in media exposure and uptake between human and chimpanzee organoids is minimal.

3.6. NEUROGENIC LENGTH OF HUMAN ORGANOID CORTICES IS LONGER THAN THAT OF CHIMPANZEE ORGANOID CORTICES:

Gliogenesis in primates overlaps with late stages of neurogenesis (Rakic, 2002) unlike in rodents where gliogenesis begins at the end of neurogenesis (Reid et al., 1995; Costa et al., 2009). The early onset of gliogenesis as early as D52 in the chimpanzee organoids is indicative of a declining neurogenic phase as shown in previous studies (Stolt et al., 2003; Martynoga et al., 2012). Interestingly enough, gliogenesis in chimpanzees appeared to have begun before the generation of the late born SATB2 positive neurons indicating that the chimpanzee organoid cortex was still between mid to late neurogenesis.

Studies at later time points such as D69, D79 showed an onset of SATB2 positive neurons in both species indicating late stages of neurogenesis, with the mature oligodendrocytic and astrocytic marker, S100β expression occurring only in chimpanzee organoid cortices but not in human organoid cortices. Ultimately, the human organoid cortices showed S100β expression at D116 indicating that the maturation of the macroglia had begun sometime within the time window of D79 and D116, in human organoids.

These observations along with the observations that the human PAX6+ progenitor cells (APs and BPs) could have a greater proliferative capacity than

chimpanzee progenitor cells, indicate than the human organoid cortex could have a longer neurogenic phase than the chimpanzee cortex resulting in a higher neuron output, thus supporting the computational prediction done by Lewitus et al., in 2014.

Further experiments aimed at quantifying the overall neuron output between human and chimpanzee cortices and lineage tracing experiments aimed at understanding the differences in the fate of the AP progeny between humans and chimpanzees could help better understand the mechanisms involved in the generation of a bigger brain in humans than in great apes.

4. Materials and methods

4.1. MATERIALS:

4.1.1. Cell lines:

Cell line	Species	Source
H9 feeder free cell line	Human	WiCell institute
409B2	Human	RIKEN BRC cell bank
SC102A-1	Human	Systems Biosciences
PR818-5	Chimpanzee	F. Gage, Salk Institute, CA
Sandra A	Chimpanzee	Svante Pääbo, Leipzig
Toba	Orangutan	Svante Pääbo, Leipzig

4.1.2. Cell culture components:

Component	Source
mTeSR1 with 5X supplement	Stem cell technologies
Rock inhibitor Y27632	VWR
Matrigel	Corning (BD biosciences)
6 well plates	Thermofisher (nunc)
6 cm dish	Thermofisher (nunc)
TrypLE express 1x (w/o phenol red)	Thermofisher (Gibco)
DMEM/F12 (Hepes)	Thermofisher (Gibco)
GlutaMAX	Thermofisher (Gibco)
Penicillin/Streptomycin	Sigma- Aldrich
MEM- NEAA	Sigma- Aldrich
2-Mercaptoethanol	Sigma- Aldrich
Heparin	Sigma- Aldrich

N2 supplement (100X)	Thermofisher (Gibco)
B27 supplement –vitamin A (50X)	Thermofisher (Gibco)
B27 supplement +vitamin A (50X)	Thermofisher (Gibco)
Insulin	Sigma- Aldrich
Neurobasal medium	Thermofisher (Gibco)
Hera cell incubator	ThermoScientific
Venor GeM Mycoplasma testing kit	Sigma- Aldrich
Anti- TRA- 1- 60 MicroBead kit	MACS Miltenyl Biotec

4.1.3. Other reagents and chemicals:

Item	Supplier
DAPI (4', 6-diamidino-2-phenylindole)	Sigma- Aldrich
EdU (5-ethynyl-2'-deoxyuridine)	Molecular Probes
Gelatin	Roth
Glycine	Merck
Glycerol	VWR
Mowiol	Calbiochem
OCT compound (TissueTek)	Sakura Finetek
Paraformaldehyde	Merck
Sucrose	Merck
Triton X- 100	Sigma- Aldrich

4.1.4. Organoid culturing solutions and media:

Solution/ Medium	Composition	Storage
Heparin (stock)	5 mg/ml heparin in PBS	–20 °C for up to 1 year
Heparin (working)	2 ml of heparin stock 8 ml DMEM/F12	–20 °C for up to 6 months
2-Mercaptoethanol (working)	1:100 dilution in DMEM/F12	
Neural Induction medium	48.5 ml DMEM/F12 0.5 ml N2 supplement 0.5 ml GlutaMAX 0.5 ml MEM-NEAA 50 µl Heparin (working)	4 °C for up to 2 weeks
Differentiation medium	125 ml DMEM/F12 125 ml Neurobasal medium 1.25 ml N2 supplement 1.25 ml MEM-NEAA 2.5 ml GlutaMAX supplement 2.5 ml B27 +/– vitamin A 2.5 ml Pen/Strep 62.5 µl Insulin 87.5 µl 2-Mercaptoethanol	4 °C for up to 2 weeks

4.1.5. Buffers and mounting media:

Solution	Components	Concentration
1X PBS (pH 7.4)	NaCl	137mM
	KCl	2.7 mM
	KH_2PO_4	1.4 mM
	Na_2HPO_4	10 mM
Tx Buffer (in 1X PBS)	NaCl	300 mM
	Gelatin	0.2%
	Triton X- 100	0.3%
Mowiol (in 6 ml H_2O)	Glycerol	6.9 g
	Mowiol	2.4 g
	200 mM Tris/HCl pH 8.5	120 µl

4.1.6. Primary antibodies:

Antigen	Host species	Description	Supplier	Dilution
Ki67	Rabbit	Polyclonal, IgG	Abcam	1:250
Pax6	Rabbit	Polyclonal, IgG	Covance	1:250
Tbr2	Sheep	Polyclonal, IgG	R&D systems	1:250
Tbr2	Chicken	Polyclonal, IgG	Merck Millipore	1:500
Vimentin (phospho S71)	Mouse	Polyclonal, IgG	MBL	1:500
Histone H3 (phospho S28)	Rat	Polyclonal, IgG	Abcam	1:200

Ctip2	Rat	Polyclonal, IgG	Abcam	1:200
SATB2	Mouse	Monoclonal, IgG	Abcam	1:200
Doublecortin C-18 (DCX)	Goat	Polyclonal, IgG	Santa Cruz	1:200
GFAP	Rabbit	Polyclonal, IgG	Dako	1:1000
S100β	Rabbit	Polyclonal, IgG	Abcam	1:500
Collagen V	Rabbit	Polyclonal, IgG	Abcam	1:250

4.1.7. Secondary antibodies:

Antigen	Host species	Conjugated fluorophore(s)	Supplier	Dilution
Mouse IgG	Donkey	Alexa Fluor® 488, 647	Molecular probes	1:500
Rabbit IgG	Donkey	Alexa Fluor® 488, 555	Molecular probes	1:500
Rat IgG	Donkey	Alexa Fluor® 488	Molecular probes	1:500
Goat IgG	Donkey	Alexa Fluor® 488, 647	Molecular probes	1:500
Sheep IgG	Donkey	Alexa Fluor® 488	Molecular probes	1:500
Chicken IgG	Donkey	Alexa Fluor® 488	Molecular probes	1:500

4.2. METHODS:

4.2.1. Cell line culturing and maintenance:

All embryonic and induced pluripotent stem cell lines were cultured on nunc six well plates coated with matrigel and maintained at 37 °C and 5% CO_2. The coating of the plates and culturing of the cell lines was carried out according to the instructions in the mTeSR1 handbook from stem cell technologies with slight modifications.

For the dissociation of cells, first, the medium was aspirated and the well was washed with 1 ml of 1X PBS1 ml of TrypLE express was used per well of a six well plate and allowed to incubate at 37 °C for a maximum of 4 minutes. A shorter incubation time was used for cell line passaging, while up to 4-5 minutes were used for dissociation of colonies into single cells. Equal amount of mTeSR1 medium was added to the well to stop the dissociation reaction. The contents of the well were then transferred to a 15 ml v-bottomed falcon tube and centrifuged at 250 g (~1100 rpm). The resulting pellet was then re-suspended in 1 ml mTeSR1 medium containing 1:100 rock inhibitor (50 µm final concentration from 5mM stock in sterile H_2O) and the cells were plated as per requirement in 2 ml of mTeSR1 medium containing 1:100 rock inhibitor. The rock inhibitor was excluded from the media during subsequent media changes.

Cell lines were regularly tested for mycoplasma using a PCR-based test (Venor GeM mycoplasma testing kit) and selected for pluritopotency using Anti- TRA- 1-60 MicroBead kit (MACS) according to the manufacturer's instructions.

4.2.2. Organoid culturing and maintenance:

4.2.2.1. Embryoid body formation:

Stem cell colonies were dissociated into single cells as described above and plated onto 96 well low attachment plates at a concentration of 9000 cells per 150 µl of mTeSR1 medium (containing 1:100 rock inhibitor), per well. The day of plating was taken as day 0 (D0). The medium was changed every other day without the addition of rock inhibitor until the formation of the germ layers (~D4 to D6, except in case of Sandra A which took anytime up to D10).

4.2.2.2. Neural Induction:

Upon germ layer differentiation, the medium was switched from mTeSR1 to the neural induction medium containing N2 supplement and heparin to direct the ectoderm towards a neural lineage. The embryoid bodies were maintained in the neural induction medium until the formation of the neuroepithelia (~5 days since neural induction). Neuroepithelial buds or folds were more apparent in some cell lines than the others.

4.2.2.3. Development of the neuroepithelium:

After the appearance of the neuroepithelium, the embryoid bodies were embedded into the matrigel. For the embedding, an empty 200 µl sterile tip box was used as a template to form concave depressions (wells) on a sterile parafilm. The embryoid bodies were then placed into these tiny wells (one embryoid body per well) and were made devoid of any remnants of the media. The matrigel drops were then added to these embryoid bodies (one drop per

embryoid body) and allowed to set at 37 °C for a minimum of 15 minutes (and maximum of 1 hour) in a 6 cm sterile cell culture grade nunc dish.

After the solidification of the matrigel, differentiation medium without vitamin A was added to the embedded embryoid bodies. The parafilm was then removed from the embedded embryoid bodies by gentle shaking or peeling action. The embedded embryoid bodies were then maintained in the differentiation medium without vitamin A for up to 7 days (to promote progenitor cell proliferation and delay their direct differentiation into neurons) after which they were switched to the same medium with the inclusion of vitamin A and maintained for the rest of the desired period on an orbital shaker at 37 °C and 5% CO_2.

NOTE: The timing of each step following the germ layer formation was kept constant for each experimental batch.

4.2.3. Organoid processing:

4.2.3.1. Organoid Fixation:

Organoids were fixed on ice for 20 minutes using 4% PFA in 120 mM phosphate buffer pH 7.4 during their initial characterization then later switched to a fixation at room temperature (RT) for 20 minutes using 1% PFA. They were then washed with 1X PBS (3x 5 minutes) and equilibrated in 30% sucrose at 4 °C overnight, mounted in Tissue-TEK optimal cutting temperature (O.C.T) compound (Sakura Finetek).

4.2.3.2. Cryosectioning:

Frozen O.C.T organoid blocks were trimmed and mounted on a cryostat holder. The cryostat blade was maintained at approximately –20/ –21 °C and the sample maintained at –19/ –20 °C. The exact cutting conditions slightly varied depending on the environmental conditions and the functioning of the cryostat.

Cryosections from each block of organoids were collected on ten Superfrost Plus microscope slides in a sequential manner such that each slide had a representative section from every region of the organoid. Care was taken to collect all cryosections from a sample (except in a few cases of accidental loss) in order to maintain the overall representation of the organoid.

The cryosections were initially of 10 µm thickness, then switched to 14 µm thickness for better preservation of the continuity of the cell processes. They were allowed to air dry for about 5 minutes after the collection of the final section on the final slide and were then stored at –80 °C or –20 °C.

4.2.4. Immunofluorescence:

All steps were carried out at room temperature unless otherwise specified. The cryosections were warmed to room temperature and rehydrated with 1X PBS (3x 5 minutes), permeabilized with 0.3% Triton X- 100 for 15 minutes, quenched with 0.1 M Glycine pH 7.4 for 15 minutes and washed with Tx buffer (3x 5 minutes). The primary antibodies were incubated in Tx buffer overnight at 4 °C, washed with the same (3x 5 minutes) and incubated with the secondary antibody and DAPI in Tx buffer for 1 hour at room temperature. The

cryosections were then washed initially with Tx buffer (3x 10 minutes) and again with 1X PBS (3x 5 minutes) and mounted with a cover slip using ProLong Gold or mowiol and stored at 4 °C in the dark.

4.2.5. Cumulative EdU labeling and detection:

EdU was added to 52 days old cerebral organoids at a final concentration of 1 µg/ml (added from a 1 mg/ml EdU stock in PBS). The organoids were supplied with fresh medium containing EdU every six hours for up to 48 hours. Organoids were then collected in triplicates at the indicated time points (1, 2, 6, 24, 30/36, 48 hours) and processed as described above.

For EdU detection, the Click-iT EdU Alexa Fluor 647 Imaging Kit (Invitrogen C10340) was used. After the final washing step of the immufluorescence protocol (with 1X PBS), the cryosections were fixed once again with 4% PFA for 20 minutes, quenched with 0.1 M Glycine pH 7.4 for 15 minutes and washed with 3% Bovine serum albumin (BSA) for 5 minutes (x3). The cryosections were then incubated at RT for 30 minutes in the EdU detection mixture (prepared according to the manufacturer's instructions), washed with 3% BSA (3x 5 minutes), then again with 1X PBS (3x 5 minutes), and mounted with a cover slip using mowiol, and stored at 4 °C in the dark. Cell cycle parameters were determined using linear regression based on the model described previously (Nowakowski et al., 1989).

4.2.6. EdU pulse chase experiment:

A one-hour pulse of EdU was given to 51 days old cerebral organoids at a final EdU concentration of 1 μg/ml (added from a 1 mg/ml EdU stock in PBS). An hour later the cerebral organoids were rinsed and cultured in fresh media for 24 and 48 hours. At the end of the 24 or 48-hour period, the cerebral organoids were fixed with 4% PFA, cryosectioned and stained with KI67 antibody along with DAPI, followed by EdU detection (as mentioned above).

4.2.7. Single cell RNA sequencing experiments and analyses:

Dissociated single cells for the single cell RNA sequencing experiments were obtained and processed from the organoids cortical regions and human foetal tissue as described in Camp, Badsha et al., 2015 and Mora-Bermúdez, Badsha et al., 2016. R- studio was used to run the principle component analysis (FactoMineR package), hierarchical clustering (stats package), differential expression analysis (SCDE package), and to construct heatmaps and dendrograms (R- developmental core team, 2010; R- studio Team, 2015). Lineage network analysis and visualizations were done using igraph implemented in R. Monocle (Trapnell et al., 2014) was used to establish pseudotime estimates and corroborate lineage relationships of cortical cells. Gene ontology enrichment analyses were performed using DAVID informatics Resources 6.7 of the National Institute of Allergy and Infectious Diseases (Huang et al., 2009). In depth details of all the analyses are described in Camp, Badsha et al., 2015 and Mora-Bermúdez, Badsha et al., 2016.

4.2.8. Image acquisition and analysis:

Images were acquired with both Zeiss LSM DuoScan (Axio Observer) and Zeiss LSM 880 Airy inverted microscope, using 10X (0.45 NA), 20X (0.8 NA) Plan-Apochromat and 63X (1.3 NA) i LCI Plan-Neofluar Imm Korr DIC objectives. The laser power, gain and offset were adjusted according to the sample. The pinhole size was set equivalent to 1 Airy unit of the 647 nm laser and optical sections of optimal thickness or single section images with a resolution of 2048 x 2048 were acquired. The images were analysed using Fiji. Quantifications were carried out in cortical regions of D28 and D52-54 cerebral organoids by counting, from the ventricular to the pial surface, either all Pax6 and Tbr2 positive and negative nuclei stained by DAPI in 50-µm and 100-µm wide fields, respectively, or all Ki67-positive cells in 100-µm wide field.

4.2.9. Statistical analysis:

Data were tabulated with Excel (Microsoft, Redmond, WA) and analysed with GraphPad Prism (La Jolla, CA). Statistical significance was calculated using the Mann–Whitney U-test. Results were interpreted as statistically significant when $p < 0.05$.

4.3. TRIED AND TESTED:

4.3.1. Other organoid media:

Various combinations of the media mentioned in the table below were used to attempt generating organoids from multiple iPSC lines. The combination that worked for the majority of lines has been mentioned in the methods section above.

Steps	Media and reagents
EB generation	(i) mTeSR1 (ii) low bFGF hESC media (Lancaster et al., 2013 protocol) (iii) Aggrewell medium (stem cell technologies)
Neural induction	(i) Neural Induction medium (Lancaster et al., 2013 protocol) (ii) STEMdiff neural induction medium (stem cell technologies)

Table 1. Media and reagents tried and tested for generating cerebral organoids.

4.3.2. Electroporation of cerebral organoid:

As a trial experiment, cerebral organoids were electroporated at D12 (when the ventricles are clearly visible) with a GFP plasmid using a pulled capillary tube connected to a rubber tubing to manually exert air pressure while the organoid was placed in a mini- electroporation chamber made in house (at voltages of around 60 mV- 80 mV). High voltage was used since the current had to pass through the liquid and not directly on the tissue.

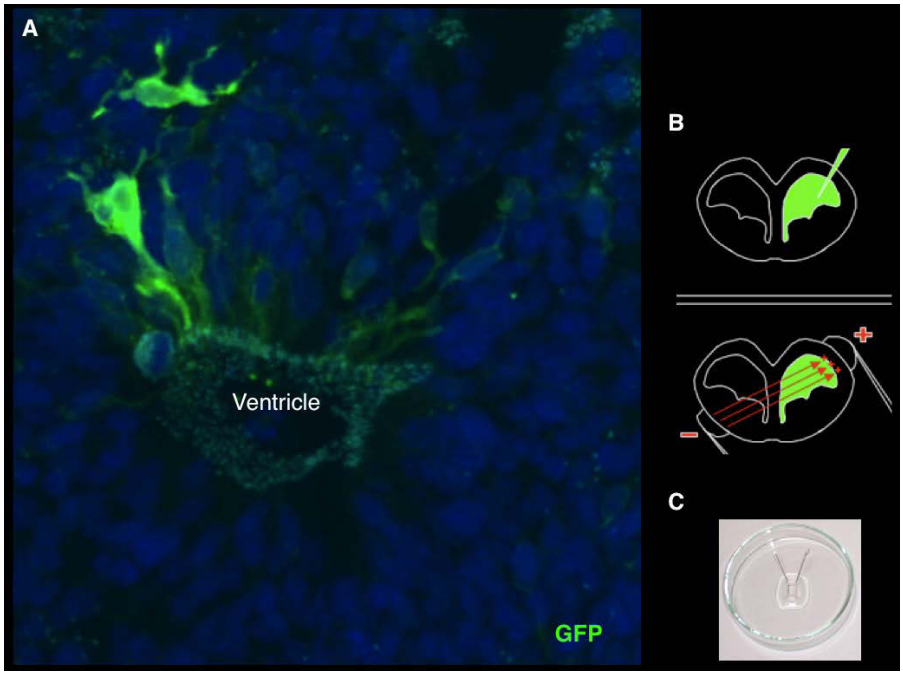

Figure 26. Electroporation of a cerebral organoid:

(A) Zoomed in image of a D12 human cerebral organoid electroporated with a control GFP plasmid from Dr. Jifeng Fei. Electroporated APs (green) are seen 24 hours after electroporation.

(B) Cartoon depiction of the electroporation of a mouse embryonic brain ventricle. GFP (green). Green arrow (above) depicts capillary used for plasmid delivery. (Below) + and – symbols with the throngs depict the electrodes. Red arrows denote direction of the current.

(C) Electroporation chamber made in house using a 6 cm glass petri dish.

5. References

Aboitiz F, Morales D, Montiel J, 2001. The inverted neurogenetic gradient of the mammalian isocortex: development and evolution. Brain Res. 38, 129- 139.

Anderson SA, Eisenstat DD, Shi L, Rubenstein JL, 1997. Interneuron migration from basal forebrain to neocortex: dependence on Dlx genes. Science 278, 474-476.

Arai Y, Pulvers JN, Haffner C, Schilling B, Nusslein I, Calegari F, Huttner WB, 2011. Neural stem and progenitor cells shorten S-phase on commitment to neuron production. Nat. Commun. 2, 154.

Betizeau M, Cortay V, Patti D, Sabina Pfister S, Gautier E, Bellemin-Ménard A, Afanassieff M, Huissoud C, Douglas R, Kennedy H, Dehay C, 2013. Precursor diversity and complexity of lineage relationships in the outer subventricular zone (OSVZ) of the primate. Neuron 80, 442-457.

Borrell V, Reillo I, 2012. Emerging roles of neural stem cells in cerebral cortex development and evolution. Dev. Neurobiol. 72, 955-971.

Borrell V, Götz M, 2014. Role of radial glial cells in cerebral cortex folding. Curr Opin Neurobiol. 27:39-46.

Bystron I, Rakic P, Molnar Z, Blakemore C, 2006. The first neurons of the human cerebral cortex. Nat. Neurosci. 9, 880-886.

Camp JG, Badsha F, Florio M, Kanton S, Gerber T, Wilsch- Brauninger M, Lewitus E, Sykes A, Hevers W, Lancaster M et al., 2015. Human cerebral organoids recapitulate gene expression programs of foetal neocortex development. Proc. Natl. Acad. Sci. U.S.A. 112:15672-15677.

Cohen E and Meininger V, 1987. Ultrastructural analysis of primary cilium in the embryonic nervous tissue of mouse. Int. J. Dev. Neurosci. 5, 43-51.

Cooper GM, 2000. The cell: A Molecular approach 2nd edition, ISBN-10: 0-87893-106-6.

Costa MR, Bucholz O, Schroeder T, Götz M, 2009. Late Origin of Glia-Restricted Progenitors in the Developing Mouse Cerebral Cortex. Cereb. Cortex 19:135-143.

Dehay C, Kennedy H, 2007. Cell-cycle control and cortical development. Nat Rev Neurosci. 8: 438-50.

Englund C, Fink A, Lau C, Pham D, Daza RA, Bulfone A, Kowalczyk T, Hevner RF, 2005. Pax6, Tbr2, and Tbr1 are expressed sequentially by radial glia, intermediate progenitor cells, and postmitotic neurons in developing neocortex. J. Neurosci. 25, 247-251.

Estivill-Torrus G, Pearson H, van Heyningen V, Price DJ, Rashbass P, 2002. Pax6 is required to regulate the cell cycle and the rate of progression from

symmetrical to asymmetrical division in mammalian cortical progenitors. Development 129, 455-466.

Farkas LM, Haffner C, Giger T, Khaitovich P, Nowick K, Birchmeier C, Paabo S, Huttner WB, 2008. Insulinoma-associated 1 has a panneurogenic role and promotes the generation and expansion of basal progenitors in the developing mouse neocortex. Neuron 60, 40-55.

Farkas LM and Huttner WB, 2008. The cell biology of neural stem and progenitor cells and its significance for their proliferation versus differentiation during mammalian brain development. Curr. Opin. Cell Biol. 20, 707-715.

Fietz SA, Kelava I, Vogt J, Wilsch-Brauninger M, Stenzel D, Fish JL, Corbeil D, Riehn A, Distler W, Nitsch R, Huttner WB, 2010. OSVZ progenitors of human and ferret neocortex are epithelial-like and expand by integrin signaling. Nat. Neurosci. 13, 690-699.

Fietz SA, Lachmann R, Brandl H, Kircher M, Samusik N, Schroder R, Lakshmanaperumal N, Henry I, Vogt J, Riehn A, Distler W, Nitsch R, Enard W, Paabo S, Huttner WB, 2012. Transcriptomes of germinal zones of human and mouse foetal neocortex suggest a role of extracellular matrix in progenitor self-renewal. Proc. Natl. Acad. Sci. U.S.A. 109, 11836-11841.

Fish JL, Kosodo Y, Enard W, Pääbo S, Huttner WB, 2006. Aspm specifically maintains symmetric proliferative divisions of neuroepithelial cells. Proc. Natl. Acad. Sci. U.S.A. 103, 10438–10443.

Florio M and Huttner WB, 2014. Neural progenitors, neurogenesis and the evolution of the neocortex. Development 141:2182-94.

Gal JS, Morozov YM, Ayoub AE, Chatterjee M, Rakic P, Haydar TF, 2006. Molecular and morphological heterogeneity of neural precursors in the mouse neocortical proliferative zones. J. Neurosci. 26, 1045-1056.

Götz M, Huttner WB, 2005. The cell biology of neurogenesis. Nat. Rev. Mol. Cell Biol. 6, 777-788.

Götz M, Stoykova A, Gruss P, 1998. Pax6 controls radial glia differentiation in the cerebral cortex. Neuron 21, 1031-1044.

Greig LC, Woodworth MB, Galazo MJ, Padmanabhan H, and Macklis JD, 2013. Molecular logic of neocortical projection neuron specification, development and diversity. Nat. Rev. Neurosci. 14, 755–769.

Groziak SM, Kirksev A, 1987. Effects of maternal dietary restriction of vitamin B6 on neocortex development in rats: B vitamin concentrations, volume, and cell estimates. J Nutr. 117:1045-52.

Groziak SM, Kirksey A, 1990. Effects of maternal restric- tion of vitamin B, on neocortex development in rats: neuron differentiation and synaptogenesis. J Nutr. 120:485-92.

Guilarte TR, 1993. Vitamin B, and Cognitive Development: Recent Research Findings from Human and Animal Studies. Nutrition Reviews 57, 7.

Hansen DV, Lui JH, Parker PR, Kriegstein AR, 2010. Neurogenic radial glia in the outer subventricular zone of human neocortex. Nature 464, 554-561.

Haubensak W, Attardo A, Denk W, Huttner WB, 2004. Neurons arise in the basal neuroepithelium of the early mammalian telencephalon: A major site of neurogenesis. Proc. Natl. Acad. Sci. U.S.A. 101, 3196-3201.

Huang da W, Sherman BT, Lempicki RA, 2009. Systematic and integrative analysis of large gene lists using DAVID bioinformatics resources. Nature Protocols 4:44–57.

Huttner WB and Brand M, 1997. Asymmetric division and polarity of neuroepithelial cells. Curr. Opin. Neurobiol. 7, 29-39.

Kadoshima T, Sakaguchi H, Nakano T, Soen M, Ando S, Eiraku M, and Sasai Y, 2013. Self-organization of axial polarity, inside-out layer pattern, and species-specific progenitor dynamics in human ES cell–derived neocortex. Proc. Natl. Acad. Sci. U.S.A. 110, 20284–20289.

Kelava I and Huttner WB, 2012. Neurogenesis in the Developing Mammalian Neocortex. In: eLS. John Wiley & Sons, Ltd: Chichester. DOI: 10.1002/9780470015902.a0022541.

Konno D, Shioi G, Shitamukai A, Mori A, Kiyonari H, Miyata T, Matsuzaki F, 2008. Neuroepithelial progenitors undergo LGN-dependent planar divisions to maintain self-renewability during mammalian neurogenesis. Nat. Cell Biol. 10, 93-101.

Kosodo Y, Röper K, Haubensak W, Marzesco AM, Corbeil D, Huttner WB, 2004. Asymmetric distribution of the apical plasma membrane during neurogenic divisions of mammalian neuroepithelial cells. EMBO J. 23, 2314- 2324.

Kowalczyk T, Pontious A, Englund C, Daza RA, Bedogni F, Hodge R, Attardo A, Bell C, Huttner WB, Hevner RF, 2009. Intermediate neuronal progenitors (basal progenitors) produce pyramidal-projection neurons for all layers of cerebral cortex. Cereb. Cortex 19:2439-50.

Kriegstein A, Alvarez-Buylla A, 2009. The glial nature of embryonic and adult neural stem cells. Annu Rev Neurosci. 32:149-84.

LaMonica BE, Lui JH, Hansen DV, Kriegstein AR, 2013. Mitotic spindle orientation predicts outer radial glial cell generation in human neocortex. Nat. Commun. 4, 1665.

Lancaster MA, Renner M, Martin CA, Wenzel D, Bicknell LS, Hurles ME, Homfray T, Penninger JM, Jackson AP, Knoblich JA, 2013. Cerebral organoids model human brain development and microcephaly. Nature 501:373-379.

Lancaster MA and Knoblich JA, 2014. Generation of cerebral organoids from human pluripotent stem cells. Nat. prot. Vol 9. No. 10.

Lancaster MA, Corsini NS, Burkard TR, Knoblich JA, 2016. Guided self-organization recapitulates tissue architecture in a bioengineered brain organoid model bioRxivdoi: http://dx.doi.org/10.1101/049346.

Landrieu P and Goffinet A, 1979. Mitotic spindle fiber orientation in relation to cell migration in the neo-cortex of normal and reeler mouse. Neurosci. Lett. 13, 69-72.

Lehtinen MK, Walsh CA, 2011. Neurogenesis at the Brain-Cerebrospinal Fluid Interface. Annu. Rev. Cell Dev. Biol. 27, 653-679.

Lewitus E, Kelava I, Kalinka AT, Tomancak P, Huttner WB, 2014. An adaptive threshold in mammalian neocortical evolution. PLoS Biol 12: e1002000. doi:10.1371/journal.pbio.1002000.

Lui JH, Hansen DV, Kriegstein AR, 2011. Development and evolution of the human neocortex. Cell 146, 18-36.

Ma T, Wang C, Wang L, Zhou X, Tian M, Zhang Q, Zhang Y, Li J, Liu Z, Cai Y, Liu F, You Y, Chen C, Campbell K, Song H, Ma L, Rubenstein JL, Yang Z, 2013. Subcortical origins of human and monkey neocortical interneurons. Nat. Neurosci. 16, 1588-1597.

Martynoga B, Drechsel D, Guillemot F, 2012. Molecular control of neurogenesis: a view from the mammalian cerebral cortex. Cold Spring Harb Perspect Biol 4: a008359.

Messier PE, 1978. Microtubules, interkinetic nuclear migration and neurulation. Experientia. 34, 289-296.

Molyneaux BJ, Arlotta P, Menezes JR, Macklis JD, 2007. Neuronal subtype specification in the cerebral cortex. Nat. Rev. Neurosci. 8, 427-437.

Mora-Bermúdez F, Badsha F, Kanton S, Camp JG, Vernot B, Kohler K, Voigt B, Okita K, Maricic T, He Z et al., 2016. Differences and similarities between human and chimpanzee neural progenitors during cerebral cortex development. Elife 5:e18683.

Noctor SC, Martinez-Cerdeno V, Ivic L, Kriegstein AR, 2004. Cortical neurons arise in symmetric and asymmetric division zones and migrate through specific phases. Nat. Neurosci. 7, 136-144.

Nowakowski RS, Lewin SB, Miller MW, 1989. Bromodeoxyuridine immunohistochemical determination of the lengths of the cell cycle and the DNA-synthetic phase for an anatomically defined population. J Neurocytol. 18: 311-8.

Otani T, Marchetto MC, Gage FH, Simons BD, Livesey FJ, 2016. 2D and 3D stem cell models of primate cortical development identify species-specific differences in progenitor behavior contributing to brain size. Cell Stem Cell 18: 467-480.

Paridaen JTML, Huttner WB, 2014. Neurogenesis during development of the vertebrate central nervous system. EMBO Reports 15, 351–364.

Rakic P, 1995. A small step for the cell, a giant leap for mankind: A hypothesis of neocortical expansion during evolution. Trends Neurosci. 18: 383–388.

Rakic P, 2002. Neurogenesis in adult primate neocortex: an evaluation of the evidence. Nature Reviews Neuroscience 3, 65-71.

Reid CB, Liang I, Walsh C, 1995. Systematic widespread clonal organization in cerebral cortex. Neuron 15: 299-310.

R Development Core Team. 2010. R: A language and environment for statistical computing. R Foundation for Statistical Computing. Vienna, Austria.

RStudioTeam. 2015. R: A language and environment for statistical computing. R Foundation for Statistical Computing. Vienna, Austria.

Salomoni P and Calegari F, 2010. Cell cycle control of mammalian neural stem cells: putting a speed limit on G1. Trends Cell Biol. 20:233-43.

Sauer FC, 1935. Mitosis in the neural tube. J. Comp. Neurol. 62, 377-405.

Smart IH, 1972a. Proliferative characteristics of the ependymal layer during the early development of the mouse diencephalon, as revealed by recording the number, location, and plane of cleavage of mitotic figures. J. Anat. 113, 109–129.

Smart IH, 1972b. Proliferative characteristics of the ependymal layer during the early development of the spinal cord in the mouse. J. Anat. 111, 365–380.

Smart IH, 1973. Proliferative characteristics of the ependymal layer during the early development of the mouse neocortex: a pilot study based on recording the number, location and plane of cleavage of mitotic figures. J. Anat. 116, 67–91.

Smart IH, Dehay C, Giroud P, Berland M, Kennedy H, 2002. Unique morphological features of the proliferative zones and postmitotic compartments of the neural epithelium giving rise to striate and extrastriate cortex in the monkey. Cereb. Cortex 12:37-53.

Smukler SR, Runciman SB, Xu S, van der Kooy D, 2006. Embryonic Stem Cells Assume a Primitive Neural Stem Cell Fate in the Absence of Extrinsic Influences. J Cell Biol. 172.1: 79–90.

Stolt CC, Lommes P, Sock E, Chaboissier M, Schedl A, Wegner M, 2003. The Sox9 transcription factor determines glial fate choice in the developing spinal cord Genes & Dev. 17:1677-1689.

Stricker SH, Meiri K and Gotz M, 2006. P-GAP-43 is enriched in horizontal cell divisions throughout rat cortical development. Cereb. Cortex 16, 121-131.

Takahashi T, Nowakowski RS, Caviness VS Jr, 1993. Cell cycle parameters and patterns of nuclear movement in the neocortical proliferative zone of the foetal mouse. J Neurosci. 13: 820-33.

Taverna E, Huttner WB, 2010. Neural progenitor nuclei IN Motion. Neuron 67, 906-914.

Trapnell C, Cacchiarelli D, Grimsby J, Pokharel P, Li S, Morse M, Lennon NJ, Livak KJ, Mikkelsen TS, Rinn JL, 2014. The dynamics and regulators of cell fate decisions are revealed by pseudotemporal ordering of single cells. Nature Biotechnology 32:381–386.

Weigmann A, Corbeil D, Hellwig A, Huttner WB, 1997. Prominin, a novel microvilli-specific polytopic membrane protein of the apical surface of epithelial

cells, is targeted to plasmalemmal protrusions of non-epithelial cells. Proc. Natl. Acad. Sci. U.S.A. 94:12425-12430.

Wilsch-Bräuninger M, Peters J, Paridaen JTML, Huttner WB, 2012. Basolateral rather than apical primary cilia on neuroepithelial cells committed to delamination. Development 139, 95-105.

6. Appendix

6.1. List of publications (from thesis work):

- Mora-Bermúdez F*, **Badsha F***, Kanton S*, Camp JG*, Vernot B, Kohler K, Voigt B, Okita K, Maricic T, He Z et al. (2016) Differences and similarities between human and chimpanzee neural progenitors during cerebral cortex development. Elife, 5:e18683.

- Camp GJ*, **Badsha F***, Florio M, Kanton S, Gerber T, Wilsch-Brauninger M, Lewitus E, Sykes A, Hevers W, Lancaster M, Knoblich J, Lachmann R, Pääbo S, Huttner WB, Treutlein B. (2015) Human cerebral organoids recapitulate gene expression programs of foetal neocortex development. PNAS: 15672– 15677, doi: 10.1073/pnas.1520760112.

* Equal contribution

6.2. List of manuscripts in preparation:

- **Badsha F** and Huttner WB, Comparison of neurogenic progression in human and chimpanzee organoid cortices.

6.3. Conference attendance:

- Cortical development conference 2014, Chania, Greece.

- ISSCR stem cell models of neural regeneration and disease 2016, Dresden, Germany.

ACKNOWLEDGEMENTS

Alhumdulillah its over! And what a ride it was!

I would first like to thank my family for their undying support, their encouragement, their love and their hard work that enabled me to get this far in life.

Yoon Jeung, Miguel- no amount of words could ever express my gratitude for you. You were my family away from home, my pillars when I needed support, my inspiration during times of difficulty.

The L14, L23 crowd- you guys are the best! I have shared some of the best times of my life with you and I continue doing so. Thank you for all your support!

My dear friend 'U' and her husband who stayed up late at nights back in their home, so I wouldn't be "alone" while writing my thesis here.

I would like to thank the Max Planck Society and MPI-CBG for this opportunity and support.

I would like to thank my TAC members and our collaborators.

I would like to thank the Huttner lab:

2016– what a year it was! Not just for me but everyone around the world. It pretty much negated everything that preceded it, and set a precedent for everything that is to come after it. I call it the year of revelations– for better or for worse.

Anger fuelled by helplessness, hatred fuelled by hypocrisy, indifference fuelled by ambition. It is during times like this that you feel the need to hold on to every little good thing within and around you– look for the good in everything when there appears to be none, look forward with hope when situations seem impossibly bleak, take time to recuperate and restore your faith in humanity.

In your lab, dear Wieland, I got to become the person I had aspired to be, (back when I had joined your lab) –more forgiving, less idealistic, more understanding and above all, I learnt to see the good in everything. The journey was tough towards the end, but I am glad I made it through. I got to see the best in me, the worst in me, and the potential of what more I could be– I also got to see the same in others. I learnt. These things may not have much to do with science, but they were valuable lessons that helped me test my own sense of integrity, loyalty and the quality of mercy. They helped me be a better person, a better

scientist. For all that and more, Wieland, I thank you. (I also thank you for the cotton candy, the multicultural food and more importantly, the lab cleaning).

Christiane, Jula, Alex, Iva, Ste and pretty much everybody else– thank you for the good times– esp Michaela, for all the timely help.

I would like to say a special thanks to my first friend here in the Huttner lab- Marta Florio. All differences aside, you were there for me during one if the toughest moments of my life, and for that I will always be grateful to you. And for everything else, I am grateful too, simply because it helped me see better, be better.

Last but not the least, I would like to thank the members of the international office, PhD office, BMS, LMF (esp my guitar teacher, Davide) and of course, the cafeteria staff!

Thank you all!

Erklärung entsprechend §5.5 der Promotionsordnung

Hiermit versichere ich, dass ich die vorliegende Arbeit ohne unzulässige Hilfe Dritter und ohne Benutzung anderer als der angegebenen Hilfsmittel angefertigt habe; die aus fremden Quellen direkt oder indirect übernommenen Gedanken sind als solche kenntlich gemacht. Die Arbeit wurde bisher weder im Inland noch im Ausland in gleicher oder ähnlicher Form einer anderen Prüfungsbehörde vorgelegt.

Die Dissertation wurde im Zeitraum vom 01.10.2012 bis 06.01.2017 verfasst und von Prof. Dr. Wieland B. Huttner, MPI-CBG betreut.

Meine Person betreffend erkläre ich hiermit, dass keine früheren erfolglosen Promotionsverfahren stattgefunden haben.

Ich erkenne die Promotionsordnung der Fakultät für Mathematik und Naturwissen- schaften, Technische Universität Dresden an.

_____

Date, Signature